IJMMM International Journal of Minerals, Metallurgy and Materials 矿物冶金与材料学报（英文版）

Process and challenges of stainless steel based bipolar plates for proton exchange membrane fuel cells

Gaoyang Liu, Faguo Hou, Shanlong Peng, Xindong Wang, and Baizeng Fang

Cite this article as:
Gaoyang Liu, Faguo Hou, Shanlong Peng, Xindong Wang, and Baizeng Fang, Process and challenges of stainless steel based bipolar plates for proton exchange membrane fuel cells, *Int. J. Miner. Metall. Mater.*, 29(2022), No. 5, pp. 1099-1119. https://doi.org/10.1007/s12613-022-2485-5

International Journal of Minerals, Metallurgy and Materials
Volume 29, Number 5, May 2022, Page 1099
https://doi.org/10.1007/s12613-022-2485-5

Invited Review

Process and challenges of stainless steel based bipolar plates for proton exchange membrane fuel cells

Gaoyang Liu[1,2),✉], *Faguo Hou*[1,2)], *Shanlong Peng*[1,2)], *Xindong Wang*[1,2)], *and Baizeng Fang*[3),✉]

1) State Key Laboratory of Advanced Metallurgy, University of Science and Technology Beijing, Beijing 100083, China
2) School of Metallurgical and Ecological Engineering, University of Science and Technology Beijing, Beijing 100083, China
3) Department of Chemical and Biological Engineering, University of British Columbia, 2360 East Mall, Vancouver, BC V6T 1Z3, Canada
(Received: 21 January 2022; revised: 1 March 2022; accepted: 28 March 2022)

Abstract: Proton exchange membrane fuel cell (PEMFC) powered automobiles have been recognized to be the ultimate solution to replace traditional fuel automobiles because of their advantages of PEMFCs such as no pollution, low temperature start-up, high energy density, and low noise. As one of the core components, the bipolar plates (BPs) play an important role in the PEMFC stack. Traditional graphite BPs and composite BPs have been criticized for their shortcomings such as low strength, high brittleness, and high processing cost. In contrast, stainless steel BPs (SSBPs) have recently attracted much attention of domestic and foreign researchers because of their excellent comprehensive performance, low cost, and diverse options for automobile applications. However, the SSBPs are prone to corrosion and passivation in the PEMFC working environment, which lead to reduced output power or premature failure. This review is aimed to summarize the corrosion and passivation mechanisms, characterizations and evaluation, and the surface modification technologies in the current SSBPs research. The non-coating and coating technical routes of SSBPs are demonstrated, such as substrate component regulation, thermal nitriding, electroplating, ion plating, chemical vapor deposition, and physical vapor deposition, etc. Alternative coating materials for SSBPs are metal coatings, metal nitride coatings, conductive polymer coatings, and polymer/carbon coatings, etc. Both the surface modification technologies can solve the corrosion resistance problem of stainless steel without affecting the contact resistance, however still facing restraints such as long-time stability, feasibility of low-cost, and mass production process. This paper is believed to enrich the knowledge of high-performance and long-life BPs applied for PEMFC automobiles.

Keywords: automobile application; proton exchange membrane fuel cell; stainless steel bipolar plates; corrosion resistance; contact resistance

1. Introduction

Proton exchange membrane fuel cell (PEMFC) automobiles are considered to be a potential solution to replace traditional fuel automobiles because of their advantages, e.g., no pollution, low temperature start-up, high energy density, and low noise. Recently, many countries have formulated the number of years for banning the sale of traditional fuel automobiles due to carbon dioxide emissions, and put PEMFC automobile into trial operation in some regions. However, due to the high cost of fuel cell related materials and components, the commercialization process of PEMFC automobiles is still a long way off [1–3].

PEMFC mainly uses perfluorosulfonic acid based solid polymer as electrolyte and commercial Pt/C or Pt–Ru/C as electrocatalysts [4–5], which are then used for the fabrication of membrane electrode assembly (MEA). Generally, hydrogen is used as fuel, oxygen or air is used as oxidant [3,6], and graphite plate or metal plate with gas flow channel is used as bipolar plates (BPs). The PEMFC stack is the core of fuel cell powered automobile engine, and the BPs are the key component of the PEMFC stack in addition to the MEA. The BPs account for more than 70% of the total weight and nearly 50% of the total cost. They are mainly used to collect conduction current, separate oxidant and reductant, and support MEA. The principle of PEMFC is shown in Fig. 1, and the specific electrochemical reaction equations are shown below [7–8]:

$$\text{Anodic reaction: } H_2 \rightarrow 2H^+ + 2e^- \quad (1)$$

$$\text{Cathodic reaction: } 1/2O_2 + 2H^+ + 2e^- \rightarrow H_2O \quad (2)$$

$$\text{Total reaction: } H_2 + 1/2O_2 \rightarrow H_2O \quad (3)$$

When the PEMFC is running, the temperature is around 60–80°C, BPs face more complex reduction (anode) and oxidation (cathode). The oxidation reaction of the anode will produce H^+, which will lead to the decrease of the pH of the electrolyte solution, and the degradation of perfluorosulfonic acid group will also produce H^+ and F^-. BP are very easy to interact with the above ions in the PEMFC, which will inevitably lead to electrochemical or chemical corrosions [6,9].

At present, the BPs materials studied are mainly divided into three categories as shown in Fig. 2 [10]: (1) graphite ma-

✉ Corresponding authors: Gaoyang Liu E-mail: liugy@ustb.edu.cn; Baizeng Fang E-mail: bfang@chbe.ubc.ca

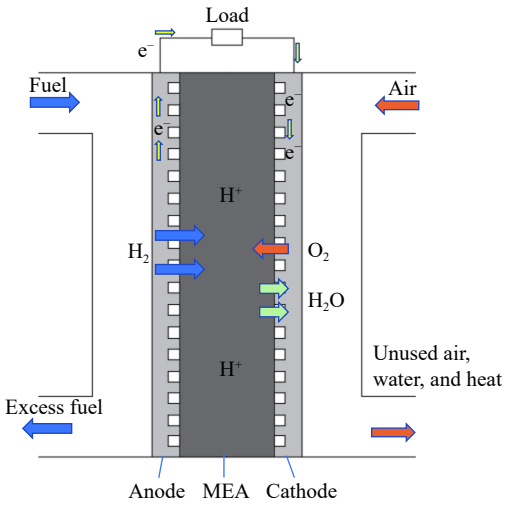

Fig. 1. Working principle of proton exchange membrane fuel cell.

terials (nonporous graphite and artificial graphite), (2) composites (polymer/carbon composites and polymer/metal composites), and (3) metal materials (coated and uncoated) [7]. Different BPs materials have different physical and chemical properties as listed in Table 1 [11].

(1) Graphite BPs.

Graphite materials include graphite, molded carbon materials, and expanded (flexible) graphite. Traditional BP are made of dense graphite (only nano and micropores) and machined into gas channels. Graphite has the advantages of excellent chemical stability, good conductivity, thermal conductivity, strong corrosion resistance, and low density [12]. However, the graphite BPs has disadvantages of high brittleness, poor strength, large limitations, and easy damage when the PEMFC is running, and the graphite material also has a large porosity, which will lead to the leakage of fuel gas and oxidizing gas. In order to ensure the strength requirements of BP and reduce gas permeability, the minimum plate thickness is 3–5 mm, resulting in lower volume specific power and specific energy density when used in vehicle applications [13].

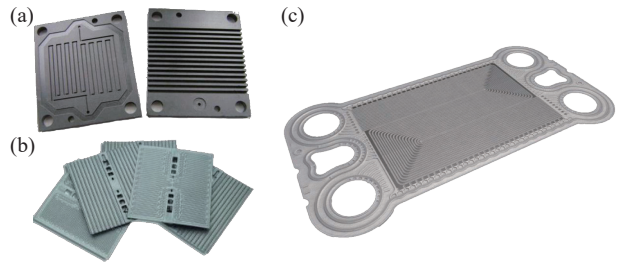

Fig. 2. BPs classification: (a) graphite BPs, (b) composite BPs, and (c) metal BPs [10].

Table 1. Comparison of physical and chemical properties of BPs of different materials [11]

BPs material	Chemical stability	Electrical conductivity	Thermal conductivity	Corrosion resistance	Mechanical strength	Machinability	Cost
Graphite BPs	Good	Good	Good	Strong	Weak	Hard	High
Metal BPs	Good	Good	Good	Weak	Good	Easy	Low
Composite BPs	Good	Fair	Fair	Strong	Good	Hard	High

(2) Composite BPs.

Composite BPs is composed of two or more materials. It has the advantages of graphite and metal BPs. It can be divided into composite structure and composite BPs. Generally, the carbon plate or graphite plate with flow field channel is prepared by injection molding or roasting process with a thin layer of metal or other high-strength conductive materials as the separation plate. It has the advantages of small volume, high strength, and good corrosion resistance, and can significantly improve the specific power of fuel cell stack. However, it also has the disadvantages of poor conductivity, poor mechanical properties, and complex manufacturing process [14].

(3) Metal BPs.

Metal BPs have become the trend of BPs research because of their low price and excellent physical and chemical properties. Aluminum, nickel, titanium, stainless steel (SS), and other metal materials can be used to produce the BPs [15–16]. The above materials not only have high strength, good plasticity, good conductivity and heat conduction ability, reduced energy loss, and good tightness which will completely separate fuel and oxidizing gas, but also are easy to process, and can be manufactured in batch with a low cost, thin thickness, and high-volume specific power, and specific energy density [7].

Overall, metal BPs can overcome some shortcomings of graphite BPs, which can be made very thin with three-dimensional channels, and thus can greatly improve the volume specific power and specific energy density of the fuel cells. The current mainstream fuel cell stacks for vehicle applications are turning to metal BPs. The development of lightweight, low-cost fuel cell metal BPs are of great significance to the performance improvement of fuel cell for vehicle applications [3].

Among all kinds of metal BPs, the industry generally believes that SS is an ideal BPs material for vehicle applications [12,17]. The advantages of using surface treated stainless steel BPs (SSBPs) are as follows: (1) the manufacturing and processing technology of SS is mature and low-cost; (2) SS with a thickness of 0.2 mm can have sufficient mechanical strength and compact structure and reduce the volume of the stack. (3) Austenitic SS containing chromium and nickel has good corrosion resistance. As listed in Table 2, austenitic SS has been applied as the BPs due to improved conductivity and corrosion resistance [18]. Previous reports also have shown that austenitic SS such as 304 and 316L are the most suitable materials for the BPs [17]. The SSBPs using stamping, high-speed laser welding, and high-performance coating have been initially used in the vehicle fuel cell system, which has greatly decreased the cost of BPs and improved the per-

formance of fuel cell vehicles [19]. Both domestic and foreign research institutions and companies have attached great importance to this and carried out extensive research. General Motors (GM), Honda, Ford, etc. have invested a lot of research efforts in metal plate fuel cells, and GM has even begun to plan to manufacture SSBPs in China to make technical reserves for large-scale manufacturing of fuel cells.

However, SSBPs are prone to corrosion in the working environment of PEMFC. Hermann *et al.* [11] studied a variety of alloy BPs such as SS, titanium, aluminum, and nickel. The results show that the release of metal ions exchanges with protons in the proton exchange membrane, increases proton conduction resistance, and affects the performance of the fuel cells. Mehta and Cooper [20] also found that dissolved metal ions will diffuse into membrane, resulting in the decrease of conductivity of membrane. In addition, the BPs near the cathode side is easy to oxidize, resulting in an increase in contact resistance. The research of Brady *et al.* [21] shows that Cr in SS can improve corrosion resistance, but the Cr_2O_3 oxide layer formed on the surface will cause large interface resistance. Corrosion products will change the hydrophobic performance of the plate surface, which causes local water on the surface of the plate to be partially enriched, hindering the transportation of reactants, and reducing the efficiency of the PEMFC [22]. In summary, the use of SS based BPs in PEMFC has an adverse impact on the MEA and other components. Therefore, it is very important to study the surface modification and coating technology of SS materials as well as the corrosion mechanism and evaluation system of SSBPs. This puts forward the urgent demand of "solving the corrosion resistance problem of SS without affecting the contact resistance" to the research field.

Table 2. Comparison of physical and chemical properties of metal BPs

BPs material	Chemical stability	Electrical conductivity	Thermal conductivity	Corrosion resistance	Mechanical strength	Machinability	Cost
Austenitic stainless steels	Good	Good	Good	Strong	Strong	Hard	Low
Ferritic stainless steels	Good	Good	Good	Weak	Weak	Hard	Low
Aluminum alloys	Weak	Good	Good	Weak	Weak	Easy	Low
Copper alloys	Good	Good	Good	Good	Weak	Easy	High
Nickel alloys	Fair	Fair	Fair	Strong	Strong	Hard	High
Titanium alloys	Good	Good	Good	Strong	Strong	Hard	High
Amorphous alloys	Good	Good	Good	Strong	Fair	Easy	High

2. Corrosion mechanism of SSBPs

The essence of metal corrosion is the process of chemical or electrochemical reactions occurring on the surface of metals due to the interaction between the material itself and the working environment, resulting in changes of the relatively stable structure of the atoms inside the metal and further changes in the properties of the metal. As shown in Fig. 3, the corrosion process and corrosion mechanisms of SSBPs are divided into three categories [23–24]: chemical corrosion, electrochemical corrosion, and physical corrosion. The corrosion forms of SS mainly include overall corrosion, intergranular corrosion, pitting corrosion, crevice corrosion, stress corrosion, corrosion fatigue, and high temperature corrosion.

2.1. Stress corrosion

SSBPs are generally obtained by cutting, stamping, and etching. The internal stress caused by stamping and cutting and the etching acid environment are important inducements for the surface defects of BPs, which inevitably lead to a variety of defects, such as vacancies, grain boundaries, dislocations, and secondary defects even with coatings. On the cathode, these micro defects will be the origin of corrosion, which lead to reduced output power or premature failure. On the cathode, these defects may capture hydrogen atoms in cathode, and make functional groups or atoms segregate around them, resulting in the increase of local oxygen or hydrogen concentration and the uneven distribution of hydrogen in the material. SS metal is prone to "hydrogen embrittlement" during long-term service in hydrogen containing environment, resulting in irreversible hydrogen damage such as internal crack and hydrogen bubble. At the same time, the contact resistance increases and the tank voltage increases. Meanwhile, during the assembly of BPs, the external stress will strengthen, and the hydrogen in the material will interact with the stress field, resulting in the origin of hydrogen embrittlement near the micro defects. Through the first principle calculation, the process of hydrogen entering the metal is simulated. It is found that the increase of isostatic pressure reduces the energy barrier that hydrogen atoms need to overcome to enter the metal subsurface, as shown in Fig. 4.

The hydrogen embrittlement of BPs needs to be solved urgently. Some studies show that the hydrogen embrittlement trend of materials is Ti > Ta > Nb > Zr > graphite [11]. Hydrogen embrittlement can be also improved by using gold-plated materials on the cathode side, but the cost is high [25].

2.2. Chemical and electrochemical corrosion

According to previously reported literatures [26–27], corrosion of the SSBPs is spread mainly by crevice corrosion and pitting corrosion. Pitting is a local corrosion that is relatively concentrated in a small part of the metal surface. Pitting corrosion of SS mainly occurs in aqueous solution containing halogen ions, such as Cl^-, Br^-, F^-, etc. and becomes especially serious in an acidic environment. Pitting corrosion is caused by the destruction of passive film by active ions. Weak parts of passive film on SS surface, such as surface

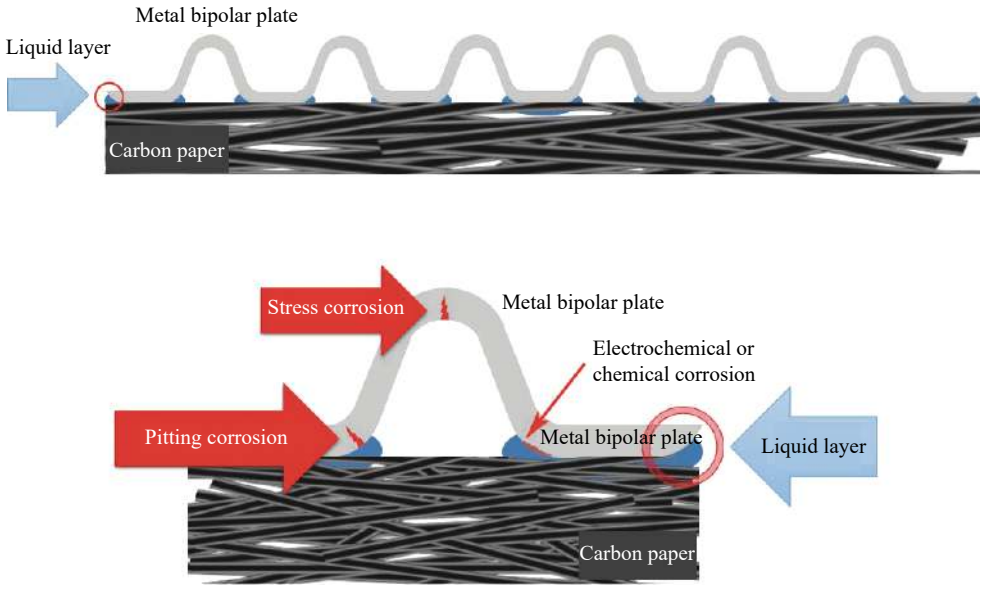

Fig. 3. Schematic diagram of metal BPs corrosion.

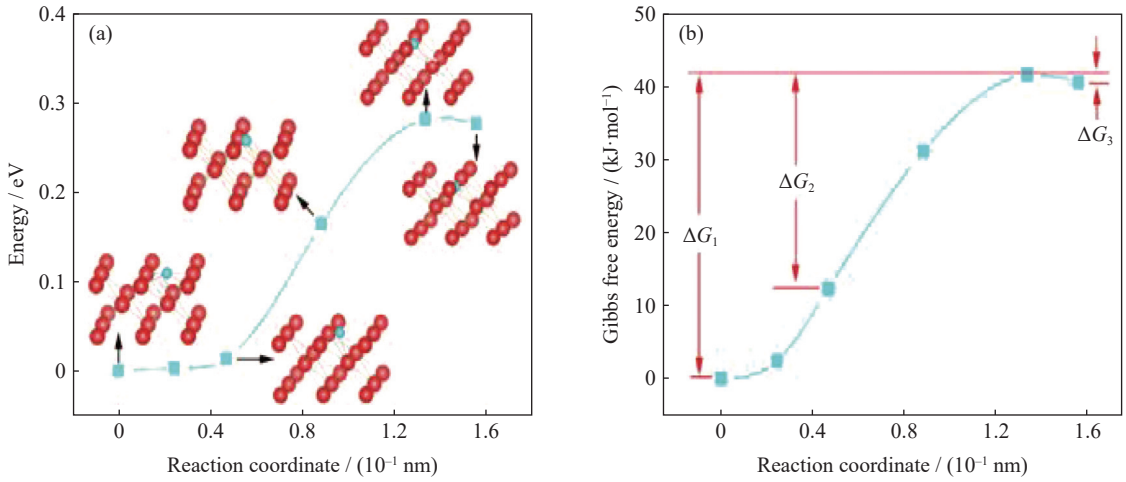

Fig. 4. Schematic diagram of the process of hydrogen entering the SSBPs: (a) results of the density functional theory calculation and the architecture of the corresponding transition state position; (b) the Gibbs free energy obtained by the Debye model.

iron particles, surface attachments, inclusions, and intermetallic compounds, are prone to pitting corrosion [28]. The rapid increase of micro "rust holes" on the surface of SS is the root cause of large-scale corrosion failure of SS, which results in a significant increase in the contact resistance, eventually causes the BPs to fail prematurely [23].

As shown in Fig. 5, the pitting process can be divided into three stages [27–29]: (1) pitting nucleation; (2) pitting growth; (3) re-passivation of etched holes. On the first stage, the aqueous solution containing halogen ions could enter the subsurface through holes or looseness. Both the chemical and micro-electrochemical corrosion occur. On the second stage, the corrosion hole will continue to develop. Both chemical and electrochemical corrosion together will result in the subsurface matrix ulceration in the pitting micro-region, and the ulcer area expands outward to peel off the coating from the substrate. The corrosion hole may turn to the third stage and stabilize due to the re-passivation film, and the corrosion hole will stop developing. Therefore, pitting control in the re-passivation stage can reduce the harm of pitting corrosion.

There are many models and theories on the development mechanisms of pitting corrosion of SS. These theories can be roughly divided into passive film damage theory and adsorption theory. Electrochemical or chemical passivation can be formed in both the non-coated and coated SSBPs. The contact resistance is significantly related to the thickness and composition of the oxidation layer. As the contact resistance increases, more thermal energy is generated and less electrical energy is output [3]. Further research found that for SSBPs, alloying elements such as nickel, chromium, and manganese have an impact on the passivation layer. However, a passivation layer will reduce the conductivity of the BPs. Thus, it is significant to control the electrochemical or chemical passivation evolution in long-term PEMFC working environment.

3. Evaluation methods of SSBPs

Table 3 shows the performance indexes that should be met by BPs used for PEMFC by the Department of Energy

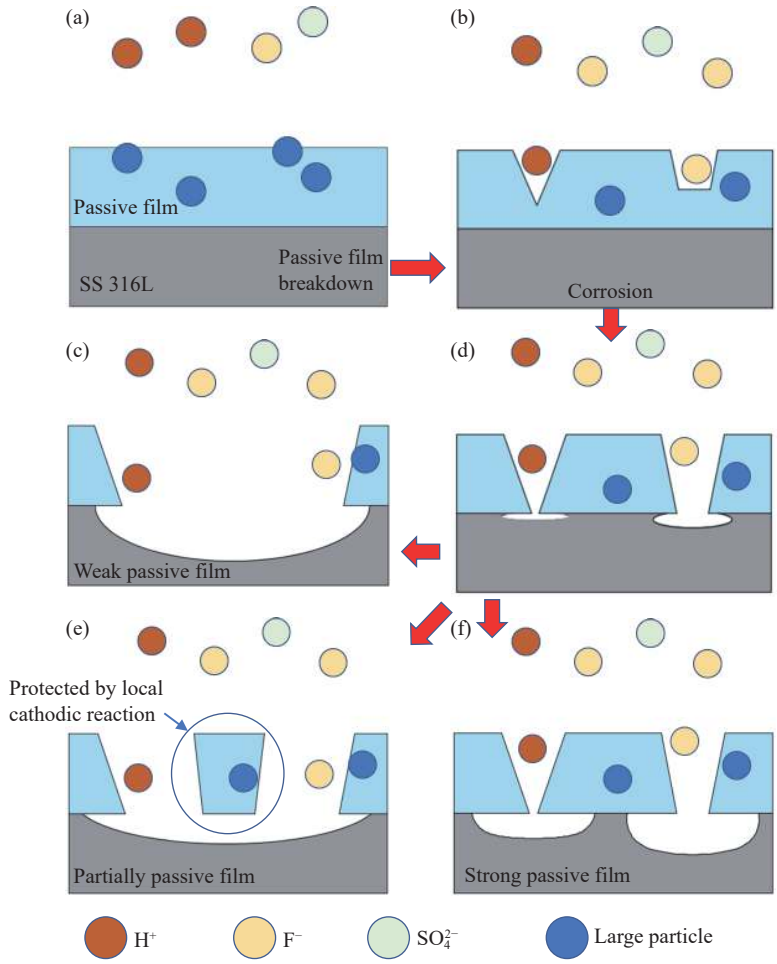

Fig. 5. Schematic diagram of corrosion mechanism of stainless steel passive film: (a) before passive film breakdown, (b) passive film damage begins. And three possibilities of (d) pitting corrosion: (c) weak passive film, (e) partially passive film, and (f) strong passive film.

Table 3. Performance index of BPs of proton exchange membrane fuel cell [15,30]

Tensile strength -ASTMD638	Flexural strength -ASTMD790	Electrical conductivity	Corrosion rate	Contact resistance	Hydrogen permeability	Mass power ratio	Density-ASTMD792	Thermal conductivity -ASTMD-256	Impact strength -ASTMD-256
>41 MPa	>59 MPa	>100 $S \cdot cm^{-1}$	<1 $\mu A \cdot cm^{-2}$	<10 $m\Omega \cdot cm^{-2}$	<2 × 10^{-6} $mol \cdot m^{-1} s^{-1} \cdot Pa^{-0.5}$	<1 $kg \cdot kW^{-1}$	<5 $g \cdot cm^{-3}$	>10 $W \cdot (m \cdot K)^{-1}$	>40.5 $J \cdot m^{-1}$

(DOE), which mainly include electrical conductivity, contact resistance, thermal conductivity, corrosion rate, hydrogen permeability, and other performance indexes [15,30]. It is noteworthy that the corrosion current density of metal BPs should be less than 1 $\mu A \cdot cm^{-2}$, while the contact resistance should be less than 10 $m\Omega \cdot cm^{-2}$. Both the evaluation methods of the corrosion properties and the contact resistance of the BPs are summarized in the review.

The pitting corrosion is the main corrosion type of the SSBPs of an actual fuel cell. Therefore, it is particularly important to evaluate the pitting corrosion. After the SSBPs are installed into the fuel cell, the fluctuation of the working current of the fuel cell far exceeds the change value of the corrosion current of the BPs. Therefore, the actual life of the BPs cannot be characterized by parameters such as corrosion current during the operation of the actual fuel cell. When the actual fuel cell is running, its power curve is affected by many factors, and the attenuation of power curve as an evaluation index of BPs life cannot be accurately explained [26]. Therefore, there are few reports on the life evaluation methods of BPs. Researchers [31–32] once adopted a special Nafion tube reference electrode and studied the corrosion behavior and life evaluation of PEMFC SSBPs. A micropore was opened in the BPs flow field, the Nafion tube was sealed at the position of the hole, and the reference electrode and the BPs formed an electrochemical system through the liquid film on the surface of the BPs. The change of corrosion potential of BPs during actual fuel cell operation was studied. Although the modified method can measure the corrosion potential to characterize the corrosion performance of the BPs, the test process and method are complex and cumbersome. In particular, this method has extremely strict requirements for seal-

ing, and is also of difficult operation and high cost. However, the advantage is that it realizes the *in-situ* measurement of the corrosion resistance parameters of the BPs during the actual fuel cell operation. As shown in Table 4, the pH value in the fuel cell environment is between 3.0–7.0, while in the cathode environment it is about 3.0–5.0 and about 5.0–7.0 in the anode environment.

3.1. Electrochemical performance test

Electrochemical performance is mainly analyzed by potentiodynamic polarization test and potentiostatic polarization test. A typical test device is shown in Fig. 6. A traditional three electrode system was used, in which graphite served as the counter electrode (CE), saturated calomel electrode as the reference electrode (RE), modified SS as the working electrode (WE), and 0.5 M H_2SO_4 + 2 ppm F^- as the electrolyte solution to simulate the solution environment of fuel cell [16].

Corrosion reactions include the transfer of electrons and ions between metals and solutions. In the absence of external potential or external power supply, the surface corrosion reaction usually occurs at the potential when the oxidation rate and reduction rate reach electrochemical equilibrium. Potentiodynamic polarization test is a means to quickly obtain the corrosion resistance of materials in corrosive solution. Before the start of potentiodynamic polarization test, the sample was stabilized at open circuit potential for about 40 min until the voltage fluctuation is less than 10 $mV \cdot s^{-1}$, the scanning speed was 0.333 $mV \cdot s^{-1}$, and the scanning voltage range was −0.1 V vs. OCP to 0.65 V vs. SCE. The equilibrium potential (corrosion potential, E_{corr}) and equilibrium current (corrosion current, i_{corr}) can be measured by electrochemical polarization test. E_{corr} and i_{corr} are widely used as indicators of corrosion resistance of materials. Typical polarization curve of bare 316L SS is shown in Fig. 7. By extrapolating the tangential lines of anode and cathode polarization curves, the corrosion current and corrosion potential can be determined, and the Tafel slope can be obtained.

Table 4. Test conditions of SSBPs in literature

Reference	Measured pH value	Notes
Work-1 [33]	3.4–7.0	Cathode, T (temperature) = 70°C, RH 100% Anode, T = 70°C, RH 100%
Work-2 [34]	3.8–5.1	T = 75–82°C, RH variable
Work-3 [35]	3.0–7.0	T = 30/60/90°C, dew point
Work-4 [36]	4.0–6.0	T = 50/70/90°C, RH = 35%/60%/100%, pH value 1.5

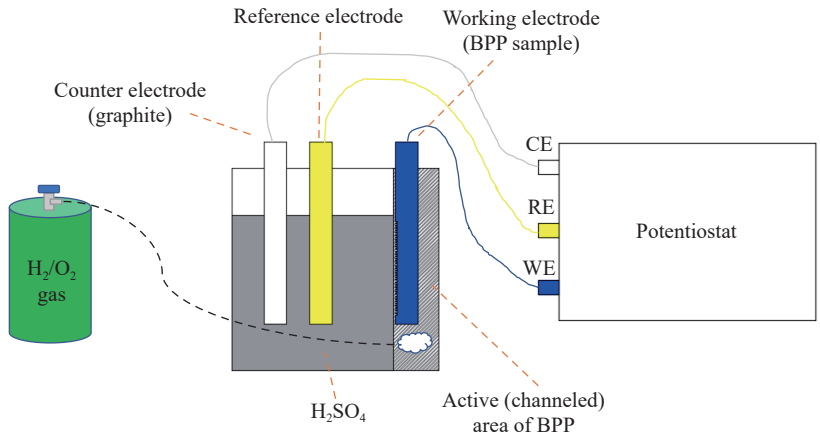

Fig. 6. Schematic diagram of three electrode system device.

Although potentiodynamic polarization test can quickly evaluate the corrosion resistance of materials, it cannot reflect the performance of materials during long-term operation. Therefore, in order to more comprehensively evaluate the long-term stability of materials in corrosive environment, the voltage under actual working conditions is applied to test the corrosion resistance of materials. In the potentiostatic polarization test, the constant temperature water bath is used to control the solution temperature of 70°C, and −0.1 V vs. SCE is applied by the electrochemical workstation in the simulated fuel cell anode environment, blowing hydrogen into the solution through the hydrogen generator for 12 h. In the simulated fuel cell cathode environment, the electrochemical

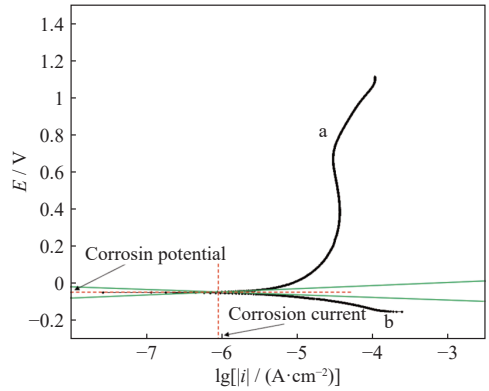

Fig. 7. Tafel fitting principle of potentiodynamic polarization curve.

workstation applies 0.6 V vs. SCE, blowing oxygen into the solution through an oxygen cylinder for 12 h [8].

Under the working conditions of PEMFC, SSBPs are prone to be corroded and dissolved. The dissolved metal ions will poison the catalysts and the membranes [15]. Thus, after the potentiostatic polarization test, the element analysis of the electrolyte solution will be necessary to measure the content of metallic ions such as Fe^{2+} released from different SSBPs. Generally, the changes of metallic ions content in electrolyte solution are analyzed by inductive coupled plasma (ICP) emission spectrometer, and the corrosion degree of SSBPs is relative with the increase of the concentration of metal ions.

Impedance technology is an advanced method to study the performance of energy devices such as fuel cells, batteries, and supercapacitors (UCS) [37]. By exploring the impedance parameters in a wide range of frequencies, the internal process of energy devices can be associated with relevant operating conditions. It can measure the response voltage by applying a small sinusoidal current signal, potentiostatic method or galvanostatic method, or vice versa. Before the test, the samples exposed to the solution were stabilized under open circuit potential (OCP) for 40 min, and then electrochemical AC impedance study (EIS) was carried out at 10 mV amplitude from 0.01 Hz to 100 kHz [8,38].

3.2. Contact resistance test

In proton exchange membrane fuel cells, BPs are usually in contact with gas diffusion layers such as carbon paper or carbon cloth. The contact resistance or interface contact resistance (ICR) should be minimized to improve the efficiency of fuel cell [39]. The ICR of the selected coating samples was tested to select the best samples for long-term corrosion test and actual fuel cell test. The measurement technology of ICR is recorded in detail in document [8,11]. The measurement scheme is described below. As shown in Fig. 8, the sample for ICR measurement (bare or coated on both sides) is located between two sheets of carbon paper, which is pressed on the sample by a pair of gold-plated metal collector plates. A controllable uniform contact pressure is applied to the metal plate at the top. The external circuit provides 1 A current to two copper plates through a constant current source, and with the gradual increase of voltage strength, a high-precision multimeter is used to measure the total voltage drop of the whole circuit under different pressures.

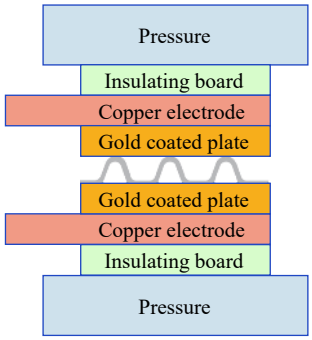

Fig. 8. Schematic diagram of ICR test.

The total resistance R_{total} in the circuit includes: (1) contact resistance $R_{Cu/C}$ between gold-plated copper plate and gas diffusion layer carbon paper, (2) contact resistance $R_{C/S}$ between carbon paper and BPs, (3) body resistance R_{Cu} of gold-plated copper plate, (4) body resistance R_C of carbon paper, (5) body resistance R_s of sample, (6) total resistance R_O of external circuit, and (7) the measurement area A of sample. Before the test, place a piece of carbon paper between two gold-plated copper plates and calculate the pre-total resistance $R_{pre\text{-}total}$ in the circuit according to Ohm's law:

$$R_{pre\text{-}total} = 2R_{Cu} + R_C + 2R_{Cu/C} + R_O \quad (4)$$

$$R_{total} = 2R_{Cu} + 2R_C + R_S + 2R_{Cu/C} + 2R_{C/S} + R_O \quad (5)$$

Compared with the contact resistance, the volume resistance of carbon paper and sample is ignored when incorporating Eq. (4) into Eq. (5), the following equations are obtained:

$$R_{C/S} = (R_{total} - R_{pre\text{-}total})/2 \quad (6)$$

$$ICR = (R_{total} - R_{pre\text{-}total})/2 \times A \quad (7)$$

3.3. Other evaluation methods

Stainless steel surface treatment technologies include non-coating or coating surface modifications. No matter which technology is adopted, microstructure (thickness, compactness, defects, etc.) and material composition (elemental composition, crystal structure, etc.) of SS surface in micron- even nano-scale closely affect the corrosion resistance and interface contact resistance of SSBPs, as well as the prediction of metal dissolution rate or residual life [23].

Scanning electron microscopy (SEM), X-ray photoelectron spectroscopy (XPS), and X-ray diffraction (XRD) were used to analyze the microstructure and composition of the coating or passive film of SSBPs, respectively. There is usually a negative correlation between corrosion resistance and interface contact resistance. Generally, SEM or transmission electron microscopy (TEM) was used to characterize the microstructure and the cross-sectional morphology of the SSBPs. The compactness and defects of the coating or passive film of SSBPs were judged from nano-scale to micro-scale, and the coating thickness could also be measured at the micro-scale even nano-scale through the cross-sectional morphology. Furthermore, energy dispersive spectrometer (EDS) was used to analyze the changes of elements before and after the surface modification of the SSBPs, and the thickness of the coating was analyzed by the changes of the relative content of elements in the cross-sectional EDS line scanning spectrum. XPS was used for qualitative and semi-quantitative analysis of the surface of the SSBPs. The information of elemental composition, chemical state, and molecular structure on the coating surface can be obtained from the peak position and peak shape of XPS spectrum, and the element content or concentration on the coating surface can be obtained from the peak intensity.

Meanwhile, it is reported that the hydrophilicity and hydrophobicity of the modified SS surface will change significantly, which will affect the gas diffusion, water management,

and electron transport of the channel field, and thus, further directly affect the performance and durability of fuel cells [20]. Contact angle test equipment is used to measure the contact angle of the droplet on the surface of the SSBPs before and after the surface modification. The contact angle can reflect the wettability properties of the SSBPs interfaces. Generally, the greater the contact angle, the more hydrophobic the SSBPs interfaces, while the smaller the contact angle, the more hydrophilic the SSBPs interfaces.

The *in-situ* electrochemical study of the coatings or passivation film stability in micro- or even nano-scale are of great significance to comprehensively evaluate the corrosion resistance of SSBPs and predict the metal dissolution rate or residual life. The *in-situ* electrochemical characterizations, e.g., EIS, cyclic voltammetry (CV), and potentiostatic polarization test, etc. were carried out in a simulated PEM fuel cell. The simulated electrolyte solution (0.5 mol·L^{-1} H_2SO_4 + 2 ppm F^-) with pure O_2 gas was pumped to simulate the cathode environment of PEMFC and high-purity H_2 gas to simulate the anode environment of PEMFC [40–41]. In addition, the changes of conductivity and pH value of electrolyte solution are monitored at regular intervals during the polarization process. At the same time, the changes of metal ions content in electrolyte solution are analyzed by ICP Emission Spectrometer. The dynamic and *in-situ* simulation of real gas-liquid mixing operating parameters in PEMFCs by adding different variables, such as different temperatures (60−80°C), different operating voltages (0.6−1.0 V), different F^- ion concentrations, and pH values on the SSBPs will significantly promote the researches and help explore the corrosion behavior and durability of different SSBPs, and provide a new standard and reference for the life test of SSBPs.

4. Surface modification technologies of SSBPs

4.1. Non-coating surface modification technologies

4.1.1. Pickling and passivation of SS

The corrosion resistance and contact resistance of SS depends largely on the composition and structure of the passivation layer formed on its surface, and the composition and structure of the passivation layer are made of SS. Several researches have shown that SS with a high content of Cr, Mo, and N have good corrosion resistance and stable output power, and both the presence of Cr and Mo is of importance for lower contact resistance [41–43]. As shown in Fig. 9, it is also confirmed that the passive film on the surface of SS is a compound of Cr. With the increase of chromium content in SS, the corrosion resistance of SS is improved. However, further work is still needed to evaluate the feasibility of low-cost, and mass production process. The natural oxide film on the surface of the SSBPs will protect the SS from further corrosion, but it will increase the contact resistance between the BPs and the electrode. If the passive film thickens with time, the contact resistance will also increase with time [28,33,44].

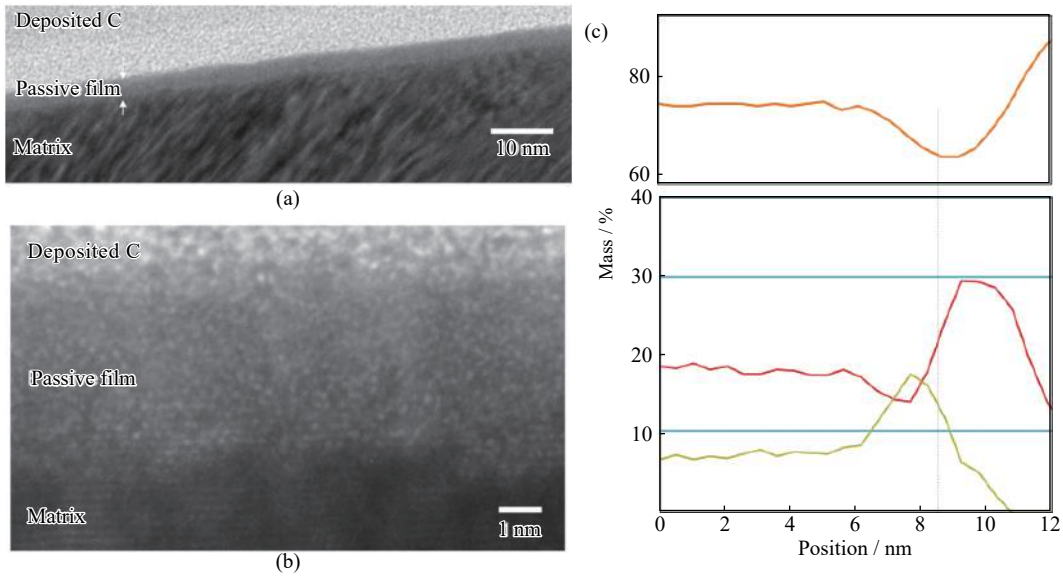

Fig. 9. (a) Cross-sectional and (b) high-resolution TEM images and (c) EDS line profiles of major matrix elements on the surface. Reprinted from *Corros. Sci.*, 52, E. Hamada, K. Yamada, M. Nagoshi, N. Makiishi, K. Sato, T. Ishii, K. Fukuda, S. Ishikawa, and T. Ujiro, Direct imaging of native passive film on stainless steel by aberration corrected STEM, 3851-3854, Copyright 2010, with permission from Elsevier.

SS treated with oxidizing medium will form uniform and dense oxide film on its surface, and the corrosion rate is significantly lower than that before treatment. The principle of passivation can be explained as follows: passivation is due to the electrochemical or chemical reaction between SS and oxidizing medium, resulting in a thin and dense oxide film with good coverage and strong adhesion on the metal surface, that is, "passivation film". Although the SS placed in the air will also have the formation of oxide film, but the protection of this film is not perfect. Generally, thorough cleaning, including alkali cleaning and pickling, and then passivation, can ensure the integrity and stability of the passivation film, and

form a complete and uniform passivation film on the surface of SS, so as to improve the aesthetics and corrosion resistance of materials and prolong the service life of SS. One of the purposes of pickling is to create favorable conditions for passivation treatment and ensure the formation of high-quality passivation film. Through pickling and passivation treatment, the oxides of iron and iron are preferentially dissolved than the chromium oxides and chromium, and the chromium poor layer is removed, resulting in the enrichment of chromium on the surface of SS, which greatly improves the stability of corrosion resistance and prolongs the time of metal rusting. The nitric acid passivation solution suitable for SS passivation is a general passivation solution, which can be prepared into nitric acid passivation solution with different proportion and concentration according to different types of SS to be passivated. The corrosion resistance and mechanism of SS nitric acid passivation film were studied in 3.5wt% NaCl solution [18]. It was found that the existence of a certain amount of hydrogen and oxygen in the film can improve the self-repair ability of the passivation film, which is an effective way to improve the corrosion resistance of SS. The passivation film is a dense oxide film composed of oxides or hydroxides of iron, chromium and nickel. As shown in Fig. 10, the main components of the inner bottom layer near the substrate interface are NiO, FeO, and Cr_2O_3, which can protect metals. Another important reason for the enhancement of pitting corrosion resistance of 316L SS after passivation is that there is excess negative charge on the passivation film surface, which shows the characteristics of p-type semiconductor, effectively preventing the diffusion and adsorption of corrosive anions in solution to the material surface [44–45].

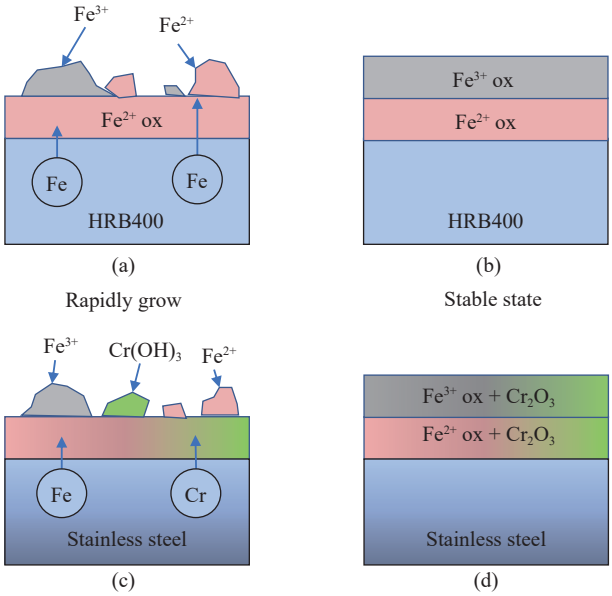

Fig. 10. Schematic diagram of passive film growth mechanism formed by HRB400 and SSS in high alkaline solution: (a) rapidly grow, (b) stable state, (c) inner layer consists of Fe^{2+} and Cr^{3+} oxides, and (d) inner layer is predominated by Fe^{2}+ oxides. Reprinted from *J. Mater. Res. Technol.*, 9, X.W. Yuan, X. Wang, Y. Cao, and H.Y. Yang, Natural passivation behavior and its influence on chloride-induced corrosion resistance of stainless steel in simulated concrete pore solution, 12378-12390, Copyright 2020, with permission from Elsevier.

The transformation of SS from activated state to passive state is a complex process. Nitric acid has strong oxidative ability, which can not only oxidize the dissolved ferrous ions and replaced hydrogen atoms, but even produce atomic oxygen. When nitric acid oxidation takes place, atomic oxygen will be chemically adsorbed on the iron surface. In chemical adsorption, atomic oxygen has the characteristics of electron absorption and metal has the characteristics of electron loss. Therefore, atomic oxygen can seize electrons from the metal to form O^{2-} ions, further form oxides and a dense oxide film on the surface of SS, which becomes a resistance layer for ion migration and diffusion, and leads to the passivation of the matrix. Similar to other passivation processes, SS must be neutralized in a weak alkaline solution after nitric acid passivation treatment to remove the local residual dilute nitric acid on the film surface to prevent its corrosion and damage to the passivation film. If neutralization treatment is not carried out, the resulting corrosion will be more serious than that without passivation treatment [46–47].

Although the stability of SS surface in corrosive medium has been improved, its matrix properties have not changed, so the passivation of SS is only a surface phenomenon. Moreover, the passivation film covers the surface of the substrate and is not constant. The outer layer of the passivation film dissolves in solution at a certain rate, and at the same time repairs the damaged surface film layer at a certain speed. Only when the repair speed is greater than or equal to the rate of dissolution, the passivation film can play a long-term protective role [45,48].

4.1.2. Electrochemical polishing of SS

Electrochemical polishing (EP) is to obtain a flat and bright surface by using the uneven dissolution caused by the difference of metal surface roughness through the electrochemical reaction process [49]. In the process of EP, the raised areas dissolve rapidly due to the ionization reaction caused by the high electric field strength. When these areas are gradually leveled, the whole surface dissolves the same, and a bright metal surface with good surface quality is obtained. Generally, the rough metal workpiece is used as the anode and the insoluble metal is used as the cathode. As shown in Fig. 11 [50], the two poles are immersed into the polishing solution of the electrolytic cell at the same time, and a current is passed to produce selective anodic dissolution, so as to achieve the effect of electrochemical modification of the surface brightness. After the metal workpiece is electrified in the electrolytic cell, many reactions will occur on the surface, mainly including metal dissolution, oxide film formation and dissolution, oxygen precipitation and other reaction processes, including: (1) discharge dissolution of metal surface elements: $Me \rightarrow Me^{n+} + ne^{-}$; (2) passive film is formed on the metal surface: $Me + nOH^{-} \rightarrow 0.5Me_2O_n + 0.5nH_2O + ne^{-}$; (3) oxygen precipitation: $4OH^{-} \rightarrow O_2 + 2H_2O + 4e^{-}$. Through the above electrochemical reaction process, the elements in the rough area of the SS surface will be pref-

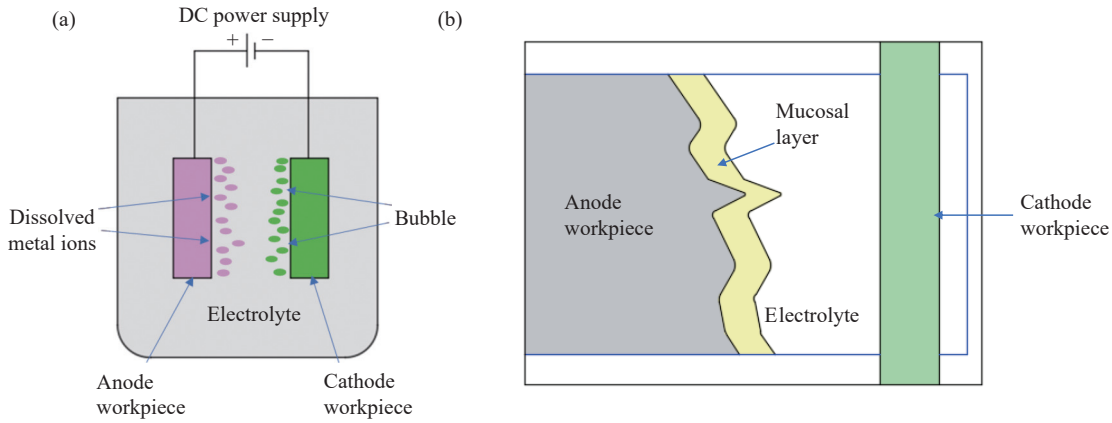

Fig. 11. (a) Schematic diagram of EP and (b) anode surface during EP. (a) [50] Reprinted from *Int. J. Mach. Tools Manuf.*, 139, W. Han and F.Z. Fang, Fundamental aspects and recent developments in electropolishing, 1-23, Copyright 2019, with permission from Elsevier.

erentially dissolved, and finally the whole surface will be bright and shiny [51].

As shown in Fig. 12, Lee and Lai [52] studied the corrosion resistance of 316L SS before and after EP. X-ray photoelectron spectroscopy (XPS) results shown in Table 5 showed that the oxide film formed by EP has significantly higher atomic Cr/Fe ratio and film thickness than the naturally grown passive oxide film formed on the surface of untreated 316L SS [49]. Due to the increase of oxide film thickness and relative Cr enrichment, the overall corrosion resistance and pitting potential of the treated 316L SS surface have been significantly improved. In addition, another reason for the improvement of corrosion resistance after EP is to remove the surface micro strain generated in the previous sample/component manufacturing and finishing processes.

The polishing quality of electropolishing surface largely depends on electropolishing parameters under the condition that the electrolyte composition is the volume mixture of sul-

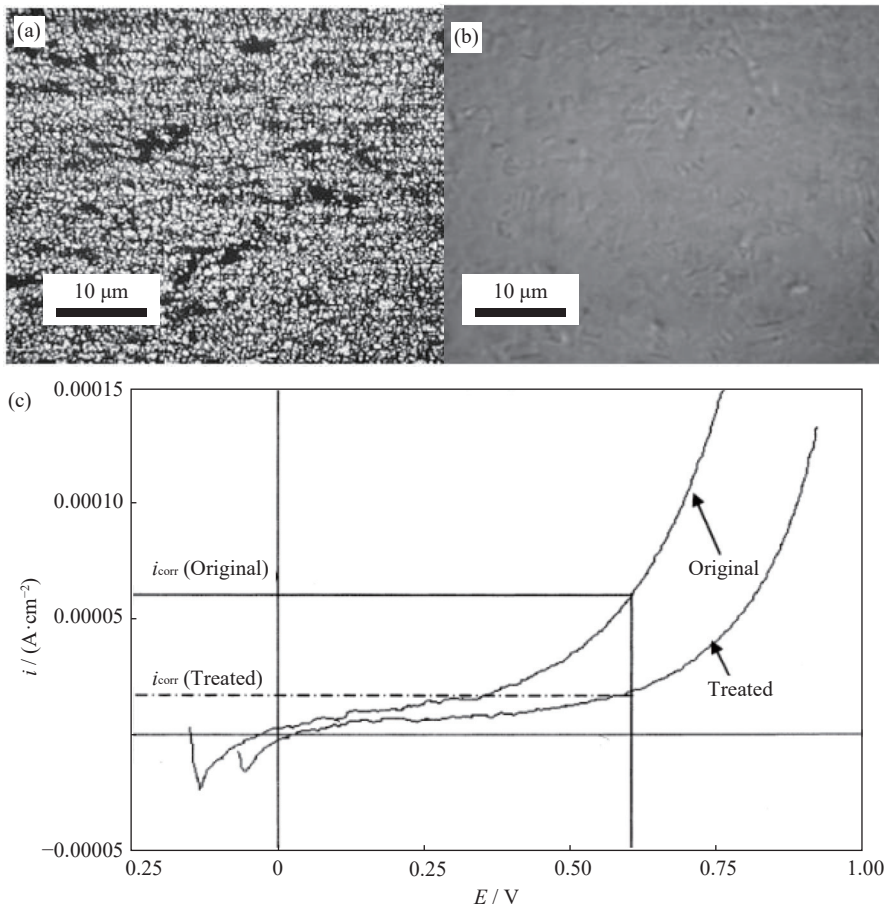

Fig. 12. Microscopy picture of (a) original specimen, (b) treated specimen, and (c) their anodic behavior in 0.5 M H_2SO_4 at 70°C. Reprinted from *J. Power Sources.*, 131, S.J. Lee, C.H. Huang, J.J. Lai, and Y.P. Chen, Corrosion-resistant component for PEM fuel cells, 162-168, Copyright 2004, with permission from Elsevier.

Table 5. XPS analysis results of SS before and after electropolishing [52]

Sample	Cr_2O_3 / wt%	FeO / wt%	Fe / wt%	Fe_2O_3 / wt%	Cr_2O_3/Fe_2O_3 ratio / wt%	Cr/Fe ratio / at%
Original specimen	24.63	6.88	0	25.4	0.97	0.76
Polished specimen	36.48	0	2.31	14.09	2.58	2.22

furic acid and phosphoric acid. Compared with the voltage and temperature parameters, the current has the greatest influence on the polishing quality of the polished surface [50–52]. Han and Fang [53] studied electropolishing of 316L SS in a sulfuric acid-free electrolyte composed of phosphoric acid, glycerol, and distilled water. It is determined that the limiting current density increases with the increase of water concentration, the material removal rate increases obviously, and the surface roughness decreases obviously. By selecting appropriate polishing conditions, the polished surface enriched with some elements can be obtained, especially for SS, which is very beneficial to the corrosion resistance and electrochemical nitriding modification of SS.

In summary, the uncoated SSBPs have significant advantages in terms of production cycles and processing costs, a series of studies have shown that their comprehensive performance still does not meet the needs of the application. In order to improve the corrosion resistance of SSBPs while maintaining their electrical conductivity, the metal substrate must be surface modified, so coated metal BPs are extensively studied.

4.2. Coating surface modification technologies

4.2.1. Electrochemical surface modification

Some noble metal (such as Au, Ag, etc.) coatings can be electrochemically deposited on SSBPs, which will undoubtedly improve the conductivity and corrosion resistance of the BPs. Wind *et al.* [15] electroplated gold coating on 316L SSBPs. The research shows that its electrochemical performance is basically no different from that of graphite BPs. However, some works found that in the initial stage, the electrochemical performance of the gold-plated BPs is similar to that of graphite, but its performance decays rapidly. Therefore, the precious metal coating technology still needs to be improved to enhance the bonding strength between the coating and the matrix alloy [54–55]. Yan *et al.* [56] treated SS by surface silver plating. The test results show that the contact resistance after modification is significantly lower than that without modification, and its performance is close to that of graphite BPs. However, the disadvantage of precious metal coating is its high cost, which is difficult to meet the requirements of commercialization, so it has little practical value.

Meanwhile, the surface composition of SS can be also electrochemically altered. As shown in Fig. 13, Wang *et al.* [57] electrochemically nitride AISI446 steel in 0.1 M HNO_3 + 0.5 M KNO_3 solution. XPS analysis showed that NH_3 was formed on the surface and a deep nitride layer was formed inside. Therefore, the surface layer of SS modified by electrochemical nitriding is composed of nitrogen-containing oxide film. Nitride steel shows very low ICR (about 18 $m\Omega \cdot cm^2$ at 140 $N \cdot cm^{-2}$) and excellent corrosion resistance in simulated PEMFC environment. Pugal *et al.* [58] formed an electrochemical nitriding surface on 316L SS by using an aqueous solution containing 0.1 M HNO_3 and 0.5 M KNO_3 at room temperature and at a constant potential. Nitrides confirmed by XPS that the formed nitrides exist in the form of mixed nitrides, CrN, Cr_2N, and nitrogen doped oxides. The corrosion behavior of untreated and nitride SS was studied in 0.5 M H_2SO_4 and 2 ppm HF. For the nitride SS, the ICR matches the value required by the DOE.

Electrochemical surface modification provides an economical way to change the surface of SS and is very promising for fuel cell BPs. Although the electrochemical surface modification treatment of SSBPs can meet the requirements of fuel cell in terms of conductivity and corrosion resistance, because the thickness of deposited layer is generally in the nanometer level, and the corrosion resistance of nitriding film has not been reported in the literature during long-time operation, it is necessary to carefully study the performance of BPs under the actual working conditions of fuel cell.

4.2.2. Vapor deposition surface modification

Currently, compound coating, e.g., transition metal carbides, nitrides and borides, etc. are mainly deposited on the surface of BPs by physical vapor deposition (PVD) and chemical vapor deposition (CVD), which can greatly improve its corrosion resistance. It is a very promising thin-layer metal plate modification method.

(1) PVD method.

The PVD method shown in Table 6 [59–60], has become the mainstream BPs surface coating modification technology due to its non-polluting environment, fast deposition rate, ability for synthesis of a variety of metal compounds and a simple process. The PVD method refers to the use of gas discharge technology under vacuum conditions, so that the target material evaporates and the evaporated material and gas are ionized, using the acceleration of the electric field, so that the resulting plasma is deposited on the substrate.

Mansoor and co-workers [61] coated a layer of alloy with good corrosion resistance (Mo ≥ 6wt%, N ≥ 21wt%, Cr ≥ 23wt%) on the surface of metal Al, and then coated a layer of TiN coating on the surface of the alloy coating. Similar to the corrosion characteristics of TiN coating on the surface of SS, this double-layer coating corrosion-resistant alloy layer will be passivated in contact with the corrosion medium of TiN layer, which improves the corrosion resistance of the whole system. The most favorable point is that it will not reduce the conductivity of the system as shown in Fig. 14. Fu *et al.* [17] plated Cr_xN coating on 316L by pulse bias arc ion plating technology. By adjusting the volume flow of nitrogen, three different coatings were obtained. It was found that the gradient film was prepared in the process of increasing the volume flow of nitrogen from 25 to 100 sccm $Cr_{0.49}N_{0.51}$–$Cr_{0.43}N_{0.57}$ coating shows good performance. When the assembly force

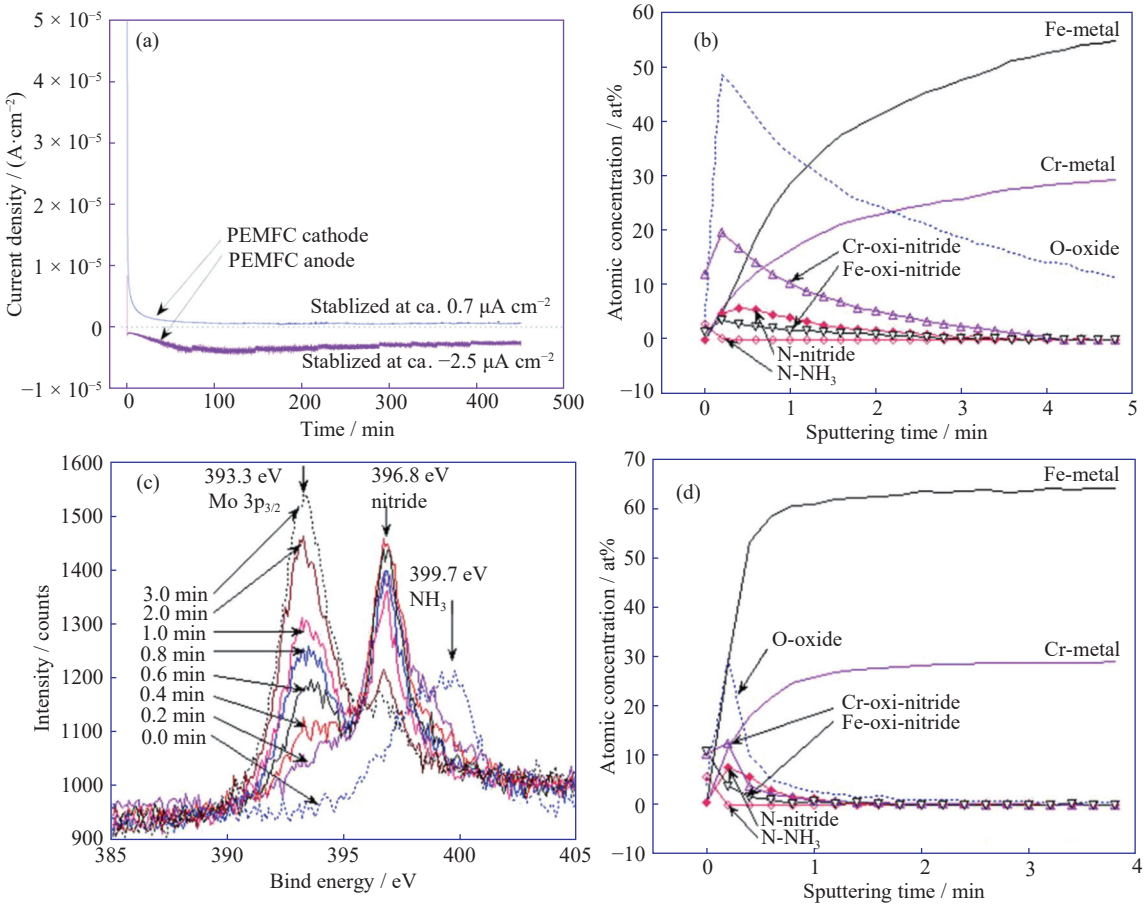

Fig. 13. AISI446 steel was electrochemically nitrided in 0.1 M HNO_3 + 0.5 M KNO_3 solution. (a) Behavior of electrochemically nitrided AISI446 steel in PEMFC anode and cathode environments. (b) XPS depth profile of electrochemical nitriding for 4 h. (c) XPS N 1s spectra of electrochemical nitriding for 4 h. (d) XPS depth profiles for electrochemically nitrided AISI446 steel after polarized 7.5 h in PEMFC anode environment. Reprinted from *Int. J. Hydrogen Energy*, 36, H.L. Wang and J.A. Turner, Electrochemical nitridation of a stainless steel for PEMFC bipolar plates, 13008-13013, Copyright 2011, with permission from Elsevier.

Table 6. Types and principle of PVD technology [59–60]

Parameter	Type	Basic process
Vacuum evaporation (heating mode)	Resistance, electron beam, laser, inductive, cathodic arc	The coating material is heated and evaporated in a vacuum container at a pressure of 1.33 × (10^{-3}–10^{-4}) Pa. The evaporated atoms or molecules are as direct as light from the evaporation source to the vaporated workpiece, and do not collide with other atoms or molecules to reach the workpiece on the way.
Sputtering deposition	High frequency induction, 2-3-4 poles, magnetic control, radio frequency magnetron, direct current sputtering, triode sputtering	Sputtering is to generate argon ion (Ar^+) by glow discharge of argon under vacuum, and bombard the cathode under the action of strong electric field, so that the atoms of cathode target are evaporated and sputtered to the substrate surface to form a film layer.
Ion plating	Resistance heating, hollow cathode, multi arc ion plating, magnetron sputtering ion plating, ion beam assisted deposition, reactive ion plating, ion cluster beam deposition	The basic characteristics of ion plating are that under low pressure (10^{-1}–10 Pa) vacuum, the gas or plating material is partially ionized by gas discharge, and then the gas or plating material ions are controlled to bombard the substrate to deposit the gas or plating material ions and their reaction products on the substrate.

is 0.8–1.2 MPa, the contact resistance is 7.9–11.2 mΩ·cm^2. The corrosion potential is 200 mV higher than that of the unmodified SS. In the simulated fuel cell working environment (0.5 mol·L^{-1} H_2SO_4 + 5 ppm F^-), the corrosion current density is 0.1 μA·cm^{-2}, the contact angle of the modified BPs is 90.5°, which is conducive to the water management of fuel cell.

(2) CVD method.

Laser CVD provides chemical vapor deposition by laser induction. It makes full use of the advantages of high laser energy density and fast heating speed, which greatly speeds up the deposition speed, low deposition temperature, and high film purity, but it cannot avoid the problem of high cost. Song *et al.* [62] prepared TiN ceramic films by this method, which has broad application prospects as shown in Fig. 15.

Plasma enhanced chemical vapor deposition (PECVD) is another surface modification technology to stimulate gas to produce low-temperature plasma and enhance the chemical activity of reactants, so as to realize the growth of thin films. It has the advantages of low deposition temperature, little influence on the substrate structure, dense film with few pin

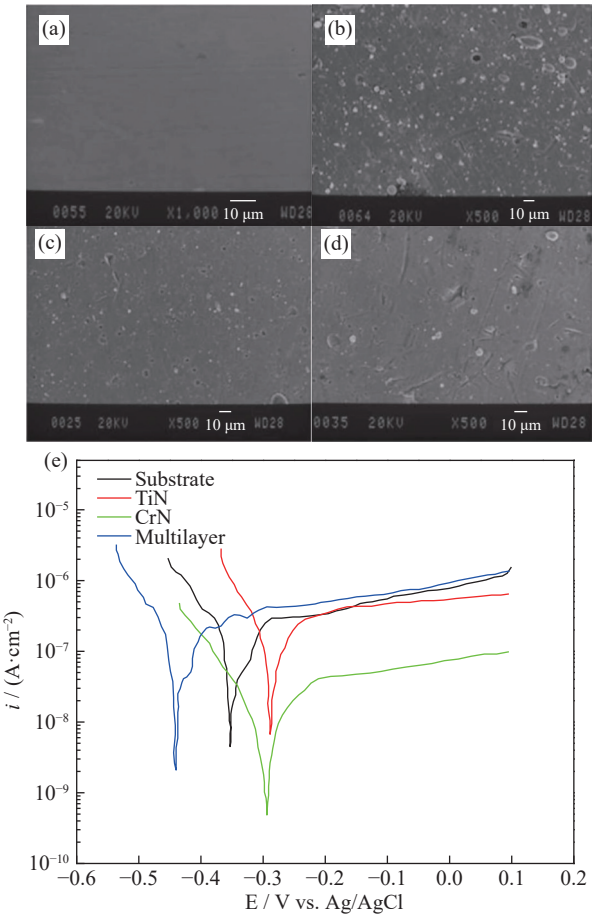

Fig. 14. SEM images of samples prepared by arc physical vapor deposition: (a) substrate, (b) TiN, (c) CrN, (d) TiN/CrN, and (e) potentiodynamic plots of substrate and coated samples. Reprinted from N.S. Mansoor, A. Fattah-Alhosseini, H. Elmkhah, and A. Shishehian, *Mater. Res. Express*, 6, art. No. 126433 (2020) [61]. © IOP Publishing. Reproduced with permission. All rights reserved.

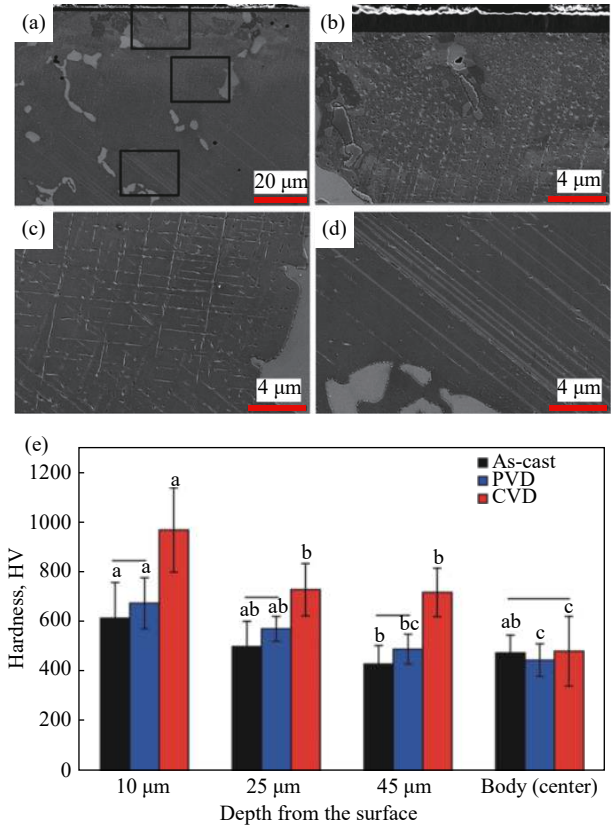

Fig. 15. Cross section SEM micrograph (a) shows CVD TiN coating and CO–Cr alloy matrix: (b–d) different distances from the coating interface and (e) nano-indentation hardness values at different depths and at the center of cross section of as-cast, PVD coated, and CVD coated alloys [62].

holes, strong adhesion between film and substrate, wide application range, etc. However, it also has the disadvantages of high cost, strong light radiation, harmful gas and so on.

In addition, CVD also includes some other chemical vapor deposition technologies, such as low pressure and atmospheric pressure, ultra-high vacuum, hot filament chemical vapor deposition, etc., which have their own advantages and disadvantages.

4.2.3. Thermochemical surface modification

Chemical surface heat treatment is also called chemical heat treatment. For a heat treatment process, steel or alloy workpieces are placed in an appropriate medium for heating and insulation so that one or more elements penetrate into its surface layer to change its chemical composition and structure in order to obtain the required properties. Carburizing, nitriding, nitrocarburizing, and carbonitriding are widely used in the surface modification of metal BPs. Thermal growth of chromium and nitride in PEMFC environment can maintain very low interface resistance. Because the thermal nitriding method is processed at a high temperature of 800–1100°C, the whole metal surface can participate in the reaction to produce a defect free surface layer.

Wang *et al.* [63] treated AISI 304 SS by thermal diffusion modification technology. Physical tests show that this method significantly reduces the ICR between SS and carbon paper, thus improving the electrochemical performance of the sample. Moreover, under the working potential of anode and cathode, the corrosion current density decreases with the increase of Cr content in the sample. However, under the condition of constant potential, the ICR is high, which cannot achieve the expected effect. Nam and Lee [64] electroplated chromium layer on the surface of 316L SS before nitriding, and studied the products under different nitriding conditions as shown in Fig. 16. It is found that increasing temperature and decreasing N_2 pressure is conducive to the formation of Cr_2N, and decreasing temperature and increasing N_2 pressure is conducive to the formation of CrN. The interfacial contact resistance and corrosion resistance of Cr_2N is better than that of Cr_2N + CrN. The metal BPs coated with Cr_2N has great potential application value.

4.2.4. Thermal spraying surface modification

Hung *et al.* [65] prepared carbide based coating on SS surface by high-speed thermal spraying technology. The fuel cell prepared with this modified BPs basically has no energy attenuation in the experimental test up to 1000 h. The results show that its output performance has great advantages compared with graphite composite BPs. Gago *et al.* [66] used this technology to prepare titanium coating on the surface of stainless steel, and systematically studied the effects of tem-

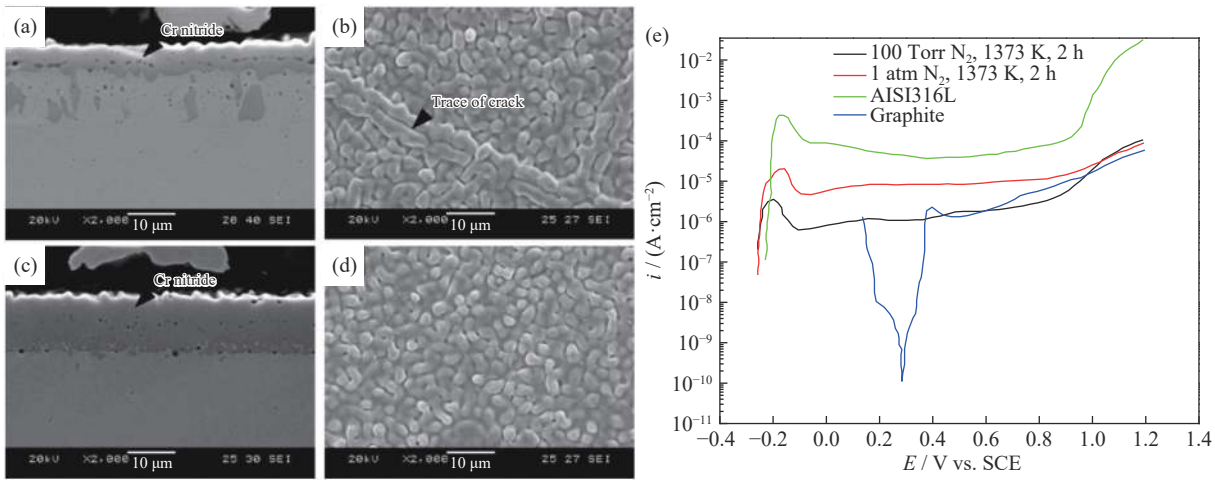

Fig. 16. SEM micrographs of the cross-section and surface of thermally nitrided AISI316L SS (a, b) in 100 Torr N_2 and (c, d) in 1 atm N_2, and (e) potentiodynamic curves for chromium nitride AISI316L SSs. Reprinted from *J. Power Sources*, 170, D.G. Nam and H.C. Lee, Thermal nitridation of chromium electroplated AISI316L stainless steel for polymer electrolyte membrane fuel cell bipolar plate, 268-274, Copyright 2007, with permission from Elsevier.

perature, nozzle type, feed rate, and other factors on the performance of BPs. It was found that titanium coating significantly reduced the corrosion current and had a good application prospect.

El-Khatib *et al.* [67] sprayed Al powder on the surface of 316L SS by supersonic spraying. The test results showed that the corrosion rate of the modified BPs was one order of magnitude lower than that of the BPs before treatment, indicating that the conductivity of the modified BPs was significantly improved. With the thickening of the coating, the corrosion rate decreases. The analysis results show that the electrochemical properties of the modified BPs may be related to the matrix composition and coating thickness, but the experimental results show that the corrosion current of the modified BPs in the cathode environment is too high, which has exceeded the application requirements of PEMFC, indicating that if the supersonic spraying method is considered to be directly applied to PEMFC, the technology of matrix composition and coating thickness still needs to be improved.

4.2.5. Ion plating surface modification

Zhang *et al.* [68] plated CrN/Cr multilayer film on 316L SS substrate by pulse bias arc ion plating as surface modified BPs. The experimental results showed that the interface conductivity of BPs plated with CrN/Cr multilayer film has been greatly improved. The results of potentiodynamic and potentiostatic tests in simulated PEMFC environment showed that the BPs plated with CrN/Cr multilayer film has good corrosion resistance.

Fu *et al.* [17] deposited a dense Cr nitride gradient film (Cr_xN) on 316L SS by pulse bias arc ion plating process. The results show that the ICR of the modified plate is 6–7 times lower than that of the untreated plate, the corrosion current is reduced by 2 orders of magnitude, and the contact angle with water is improved as shown in Fig. 17. The modified 316L SS shows good corrosion resistance. It is proved that nitride gradient film can not only significantly improve the conductivity and corrosion resistance of SSBPs, but also reduce the surface energy of the sample.

4.2.6. High energy micro arc alloying surface modification

Ren *et al.* [69] prepared a dense TiC coating on 304 SS

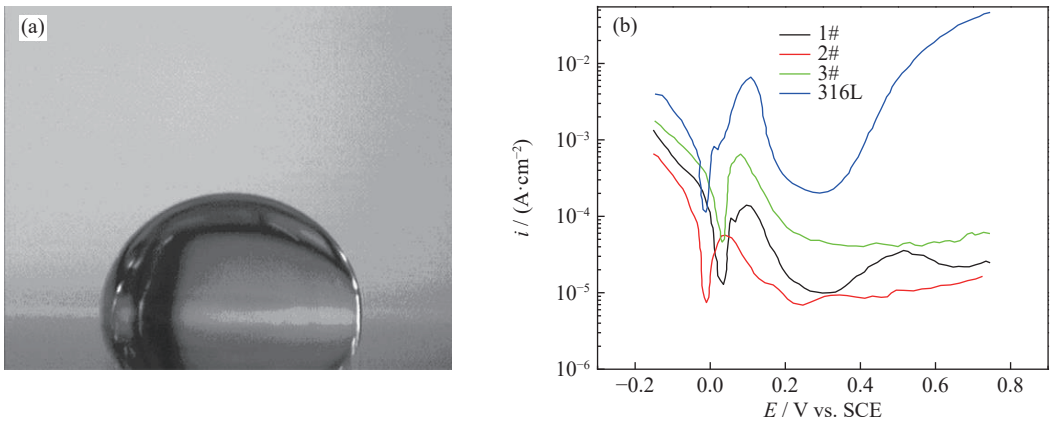

Fig. 17. (a) Dense chromium nitride films were prepared on 316L stainless steel by pulsed bias arc ion plating. (b) Potentiodynamic polarization curves of different samples. Reprinted from *J. Power Sources*, 176, Y. Fu, M. Hou, G.Q. Lin, J.B. Hou, Z.G. Shao, and B.L. Yi, Coated 316L stainless steel with Cr_xN film as bipolar plate for PEMFC prepared by pulsed bias arc ion plating, 282-286, Copyright 2008, with permission from Elsevier.

by high energy micro arc alloying technology. The process has the advantages of low cost and simple operation. Due to the metallurgical bonding, the bonding force between the base metal and the surface coating is very strong, and the properties of the coating and the substrate are similar due to their small heat affected zone. The test results show that the coating still maintains high corrosion resistance stability after soaking in 1 M H_2SO_4 solution for 30 d. The experimental results measured at PEMFC cathode working potential also show that the coating has good corrosion resistive stability.

5. Surface coating materials of SSBPs

5.1. Carbon materials

Fu *et al.* [70] prepared three different carbon based coatings on 316L SS by pulse bias arc ion plating: pure C layer, Cr–C layer, and C–Cr–N layer. Through the tests, it was found that the contact resistance between the pure C layer and C–Cr–N layer was too large, while the SS modified by C–Cr showed the best conductivity and corrosion resistance. Under the assembly force of 0.2–1.5 MPa, the contact resistance is 6.86–8.72 mΩ·cm^2. In the simulated fuel cell working environment (0.5 M H_2SO_4 + 5 ppm F^-, 25°C), the SS coated with C–Cr was subjected to potential polarization test. It was found that passivation occurred at 0.1–0.8 V vs. SCE, and the passivation current density was 0.1 μA·cm^{-2}, which is 2 orders of magnitude lower than that of the untreated SS. The passivation current density increased to 101.25 μA·cm^{-2} in air atmosphere at 70°C.

Feng *et al.* [71] prepared 3 μm thick dense amorphous carbon layer on 316L SS by closed field balanced magnetron sputtering ion plating. When the assembly force was 1.2–2.1 MPa, the contact resistance was 8.3–5.2 mΩ·cm^2, while the contact resistance of graphite was 10.4–5.4 mΩ·cm^2. The anode passivation current density was 3.56 μA·cm^{-2} after the potential test under the simulated fuel cell working environment (0.5 M H_2SO_4 + 2 ppm HF, 80°C), and the cathode polarization current density was 2.4 μA·cm^{-2} after the polarization test under constant potential for 8 h, but it was always in a protective state under the anode environment. At the same time, Yi *et al.* [12] prepared an amorphous carbon layer on 304 SS by the same method, made BPs with the modified SS, assembled into 40 cm^2 single cell, and investigated the performance and durability of the stack as shown in Fig. 18. The test results of single cell showed that when the cell voltage was 0.6 V, its output power was 923.9 mW·cm^{-2}, which was 3.02 times that of the unmodified 304 SSBPs cell, The maximum power density of the modified cell was 1150.6 mW·cm^{-2}. After 200 h test, it was found that the performance degradation of single cell with the modified BPs was only 1/7 of that of the single cell with the unmodified BPs. In

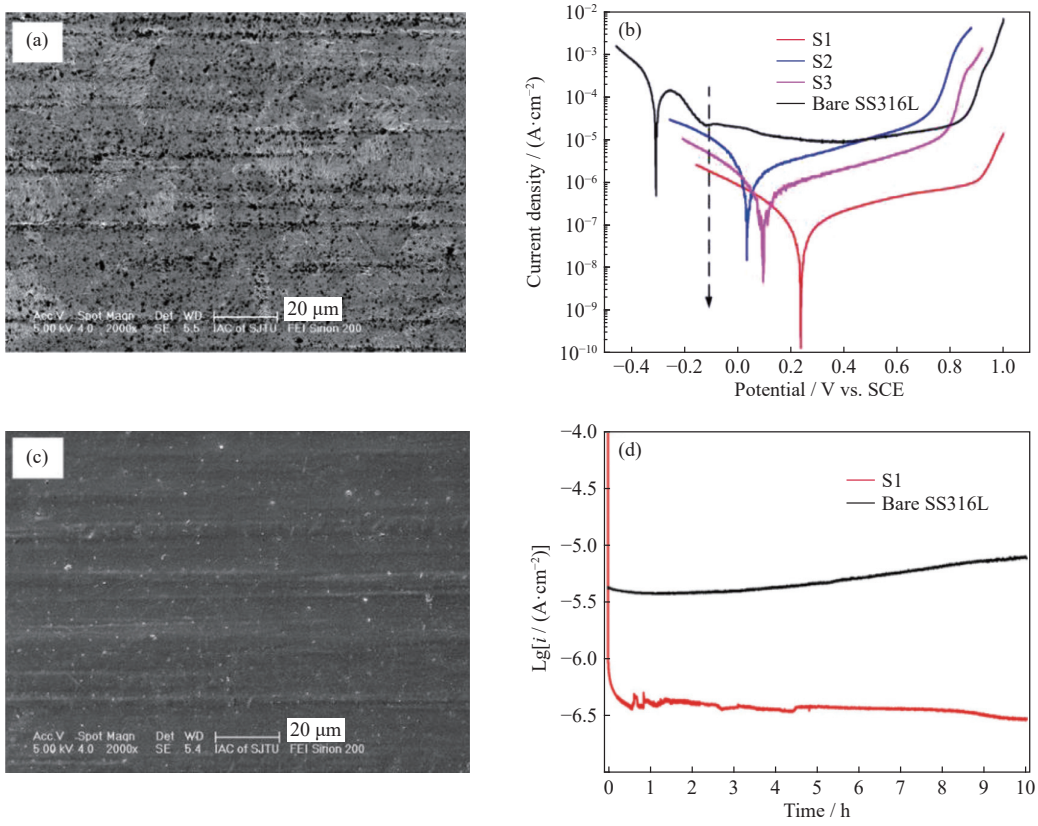

Fig. 18. Surface morphology of bare SS316L (a) and crenec coated SS316L (b) samples as anode after potentiostatic test in simulated PEMFs environment. (c) Polarization curves of the bare and Cr–N–C coated SS316L samples. (d) Potentiostatic curves acquired from the bare and Cr–N-coated SS316L samples as simulated anodic. Reprinted from *J. Power Sources*, 236, P.Y. Yi, L.F. Peng, T. Zhou, J.Q. Huang, and X.M. Lai, Composition optimization of multilayered chromium-nitride-carbon film on 316L stainless steel as bipolar plates for proton exchange membrane fuel cells, 47, Copyright 2013, with permission from Elsevier.

the performance test of 100 W short reactor, the output power density was 873.3 mW·cm^{-2} at 1.8 V. Through 48 h durability test, the stack maintained good stability.

Lee *et al.* [72] prepared C60 nanographite coating on 316L SS by ion plating method, and its contact resistance was measred to be 12 mΩ·cm^2 under the assembly force of 150 N·cm^{-2}, which remained low contact resistance even after the corrosion test. The potentiodynamic test was carried out in a simulated fuel cell working environment (0.5 M H_2SO_4 + 2 ppm HF, 80°C), and the corrosion current density was 0.05 μA·cm^{-2} under the hydrogen supply of the anode, which was two orders of magnitude lower than that of the unmodified SS. The corrosion current density of the cathode under air was 0.23 μA·cm^{-2}. Under the potentiostatic polarization test, the modified SS still showed good corrosion resistance.

5.2. Metal materials

In addition to the electrochemically deposited noble metals on SS mentioned above, niobium, nickel, etc. have also been used for coating materials. Wang *et al.* [73] and Weil *et al.* [74] proposed a concept of rolling coating of materials and plated niobium on 304 SS. It was found that the niobium coating on the surface of 304 SS formed oxide and was passivated under acidic conditions, so it had good corrosion resistance. The research shows that the metal coated materials are expected to reach DOE corrosion rate technical index 1 μA·cm^{-2} as shown in Fig. 19. Feng *et al.* [75] plated niobium on 316L SS by ion implantation technology. The ion implantation time was 0.5 h, 2 h, and 5 h. Under the simulated working environment of proton exchange membrane fuel cell (0.5 M H_2SO_4 + 2 ppm HF, 80°C), the SS after ion implantation for 2 h showed the best performance. The passivation current density under potentiodynamic test was 6 μA·cm^{-2}. After 8 hours of potentiostatic polarization test of −0.1 V vs. SCE simulated cathode, the polarization current density was 0.03–0.07 μA·cm^{-2}. However, when the assembly pressure was 1.5 MPa, the contact resistance was greater than 200 mΩ·cm^2. At the same time, Feng *et al.* [76] implanted nickel ion into 316L SSBPs by ion implantation technology. After the modification, the corrosion resistance of SS was enhanced and its contact resistance was reduced. Especially when the nickel ion implantation dose was 3 × 10^{-7} cm^{-2}, the corrosion potential increased from −0.3 V to −0.05 V under the simulated fuel cell working environment, and the passivation current density decreased from 11.26 to 7 μA·cm^{-2} at the cathode potential of 0.6 V. Although the contact resistance was reduced, it is still higher than the technical index of DOE of 10 mΩ·cm^2. With the increase of injection dose, the defects of nickel rich layer became more and

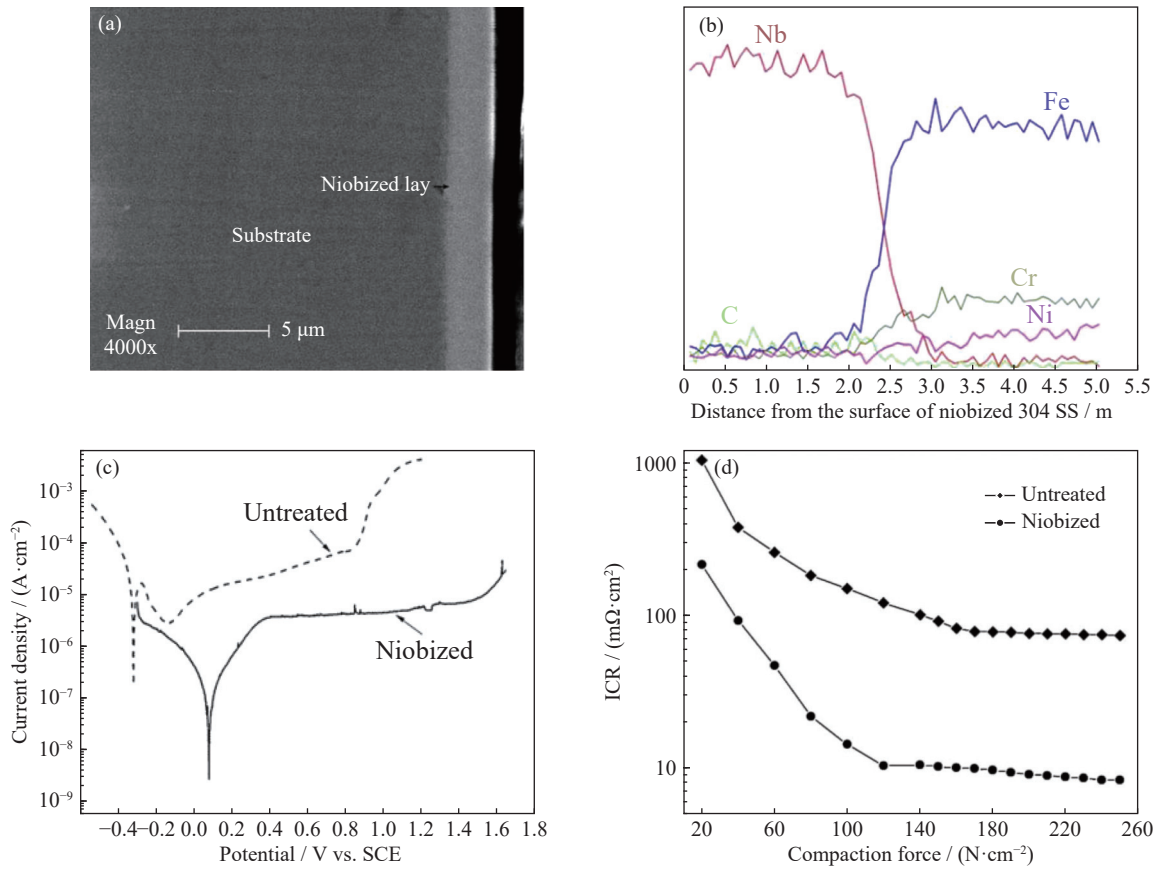

Fig. 19. (a) SEM micrograph of the cross-section for the niobized 304 SS by plasma surface diffusion alloying. (b) Elemental EDS analysis for the niobized layer. (c) Potentiodynamic polarization curves of the untreated and niobized 304 SS in 0.05 M H_2SO_4 + 2 ppm F^- solution at 70°C purged with H_2. (d) ICR of the untreated 304SS and niobized 304 SS under different compression forces. Reprinted from *J. Power Sources*, 208, L.X. Wang, J.C. Sun, P.B. Li, B. Jing, S. Li, Z.S. Wen, and S.J. Ji, Niobized AISI 304 stainless steel bipolar plate for proton exchange membrane fuel cell, 397-403, Copyright 2012, with permission from Elsevier.

more obvious, the corrosion current density increased, and the corrosion resistance decreased.

5.3. Metal carbon/nitrogen materials

The nitrogen/carbide of many transition metal elements such as titanium and chromium have good corrosion resistance and high conductivity. Recently, they have been applied to the surface modification of SS matrix by researchers.

5.3.1. Nitrogen/titanium carbide materials

Li *et al.* [77] carried out electrochemical tests on the 316L SS plated with TiN. In the simulated PEMFC environment, it was found that a small part of TiN coating was eroded after 1000 h of oxygen and 240 h of hydrogen, while the untreated 316L SS was passivated in both cases. TiN coating showed good corrosion resistance and conductivity. Cho *et al.* [78] carried out similar work. Firstly, the flow channel was etched on 316L SS by chemical etching, and then TiN coating was prepared by hollow cathode discharge ion plating. The TiN modified 316L SSBPs, unmodified 316 SSBPs, and graphite BPs were assembled into a single cell to compare the fuel cell performance. When the initial voltage was 0.6 V, the current densities of the cells were 996, 796, 896 mA·cm^{-2}, respectively. Compared with the unmodified BPs, the service life of the BPs modified by TiN is significantly longer, and the contact resistance of the modified 316 BPs is close to that of the graphite BPs. Wang and Northwood [79] prepared 15 μm thick TiN coating on 316L SS by plasma enhanced PVD technology as shown in Fig. 20. After the modification, the corrosion potential increased from −0.26 V vs. SCE to 0.16 V vs. SCE. Under the simulated anode environment (0.5 M H_2SO_4, 70°C, hydrogen atmosphere), the corrosion current density at a constant potential of −0.1 V decreased from − 10 to −40 μA·cm^{-2}, but the cathode corrosion current density increased from 5 to 25 μA·cm^{-2} at 0.6 V constant potential. SEM analysis showed that pitting corrosion occurred on the surface of the sample, resulting in serious local corrosion. At the same time, the contact resistance reached 100 mΩ·cm^2 when the assembly force was 1.56 MPa.

5.3.2. Nitrogen/chromium carbide materials

Fu *et al.* [17] plated Cr_xN and TiAlN coating on 316L by pulse bias arc ion plating technology. By adjusting the volume flow of nitrogen, three different coatings were obtained. It was found that the gradient film $Cr_{0.49}N_{0.51}$–$Cr_{0.43}N_{0.57}$ coating prepared in the process of increasing the volume flow of nitrogen from 25 to 100 sccm showed good performance. In the process of assembly force of 0.8–1.2 MPa, the contact resistance was 7.9–11.2 mΩ·cm^2. The corrosion potential was 200 mV higher than that of the unmodified SS. In the simulated cell working environment (0.5 M H_2SO_4 + 5 ppm F^-), the corrosion current density was 0.1 μA·cm^{-2}, and the contact angle of modified BPs was 90.5°, which was conducive to the water management of fuel cell. You *et al.* [80] also investageted the effect of cermet substrate characteristics on the microstructure and properties of TiAlN coatings. Zhao *et al.* [81] systematically studied the corrosion behavior of SSBPs after chromium carbide plating in simulated cell working environment. The XPS test results showed that Cr_3C_2, Cr_2O_3, FeOOH, and other substances were formed on the surface of chromium carbide plated SS, forming a dense barrier layer, which improved the corrosion resistance of 316L SS to a certain extent. In the simulated

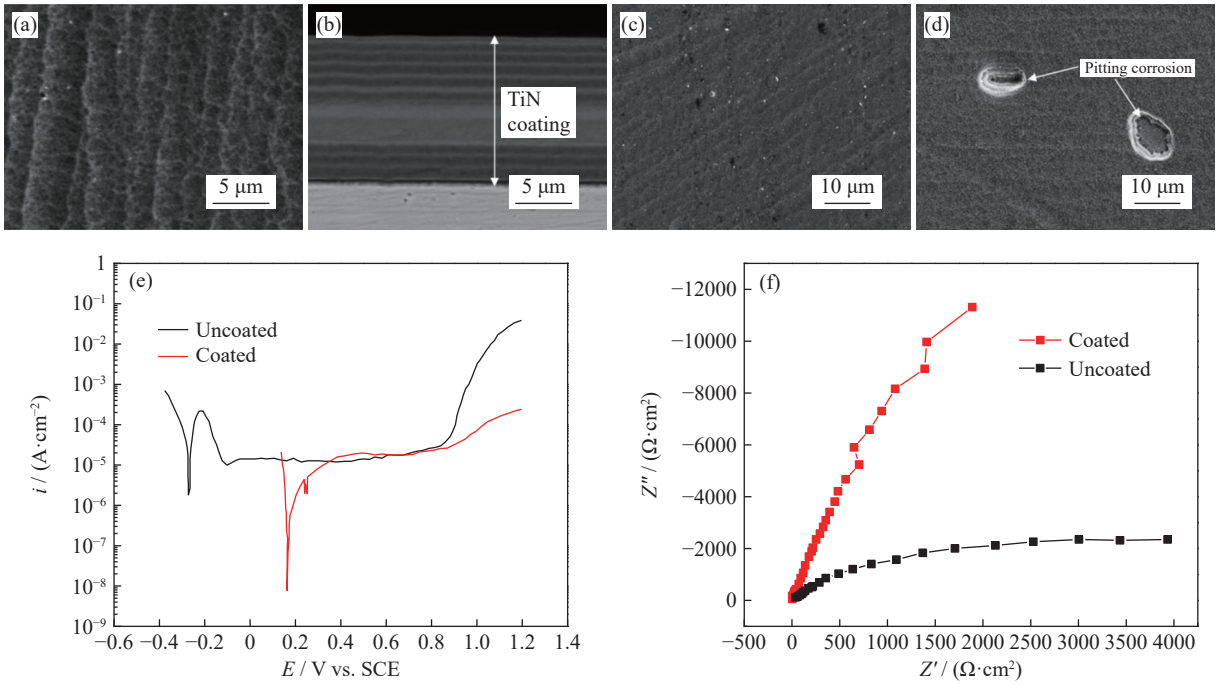

Fig. 20. (a) TiN coated SS316L TiN coating surface (secondary electron image). (b) Cross-sectional view of TiN coating on SS316L (back-scattered electron image), SEM micrographs for the coated SS316L after potentiostatic tests in the simulated anode and cathode conditions at (c) anode side and (d) cathod side. (e) Potentiodynamic tests and (f) Nyquist plots for the uncoated and TiN-coated SS316L at 70°C. Reprinted from *J. Power Sources*, 165, Y. Wang and D.O. Northwood, An investigation into TiN-coated 316L stainless steel as a bipolar plate material for PEM fuel cells, 293-298, Copyright 2007, with permission from Elsevier.

fuel cell anode environment, its pitting potential was 0.7 V. After the modification, its pitting corrosion resistance was improved. In the simulated fuel cell cathode working environment, pitting corrosion occured, and it was verified that the development rate of pitting corrosion was controlled by the dissolution of surface coating.

5.4. Conductive polymer materials

Since DeBerry [40] applied polyaniline coating to the surface of SS in 1985, conductive polymer materials have attracted more and more attention because of their high conductivity and good corrosion resistance.

Zhang and Zeng [82] studied the corrosion behavior of polypyrrole coating doped with sodium dodecyl sulfate in simulated PEMFC environment. Joseph *et al.* [83] prepared polypyrrole and polyaniline coatings on 304 SS by electrochemical deposition. It was found that 304 SS coated with polymer showed low corrosion current density, and the contact resistance was very close to graphite material under certain assembly force. However, there is no data to show the changes of coating properties under a long-term test. García and Smit [84] found that although the 304 SSBPs plated with polypyrrole had excellent corrosion resistance and the corrosion current density could be reduced to 0.2 $\mu A \cdot cm^{-2}$, with the increase of time, SEM analysis showed that the coating decomposed and then the corrosion current density increased. Wang and Northwood [85] first sprayed gold on the surface of 316L SS, and then prepared polypyrrole coating by electrochemical deposition. The potential test was carried out under the simulated fuel cell working environment, and the corrosion current density was 5.46 $\mu A \cdot cm^{-2}$. At the cathode constant potential of 0.6 V vs. SCE, the polarization current density was about 7 $\mu A \cdot cm^{-2}$. At the anode constant potential of −0.1 V vs. SCE, the modified steel plate was in cathodic protection state. Although the corrosion resistance of conductive polymer coating is good in a short time, due to the defects of polymer coating, its actual corrosion resistance in fuel cell environment needs to be investigated for a long time.

6. Conclusions and perspectives

Currently, proton exchange membrane fuel cell (PEMFC) automobiles have attracted the attentions of major automobile manufacturers and R&D institutions with their high efficiency and near-zero emissions. While, price and life are the two important factors that have plagued the industrialization of PEMFC for a long time. Especially for the bipolar plates (BPs) and their coating are very important. Even now, the graphite BPs dominate the traditional PEMFC products. The stainless steel bipolar plates (SSBPs) can greatly improve the power density and performance of PEMFC, and reduce mass production costs, which is favored by PEMFC automobile companies. The working environment of SSBPs for PEMFC is very harsh, which seriously affects its corrosion resistance and conductivity, and their working stability can be improved by changing the material composition and surface modification. Presently, the surface modification technologies mainly include both the non-coating and coating technical routes based on SSBPs, e.g., substrate component regulation, thermal nitriding, electroplating, ion plating, chemical vapor deposition, and physical vapor deposition, etc. And the surface coating materials mainly include e.g., metal coatings, metal nitride coatings, conductive polymer coatings, and polymer/carbon coatings, etc. In general, the development trend of SSBPs technology has gradually become a hotspot in research from the traditional monometallic film layer to the direction of multi-component and composite, especially the composite film layer prepared by combining metal and carbon materials. It is worth pointing out that the quality evaluation system of SSBPs after surface modification and coating is of importance. The performance and life of SSBPs mainly depend on the corrosion resistance of the plates. Except for a few precious metals, the corrosion resistance of most metals and alloys (such as chromium, nickel-chromium alloys, stainless steel, etc.) depends on the protective effect of the passivation film formed on their surfaces. Thus, not only the standard characterization of the corrosion resistance and interface contact resistance of SSBPs, but also further analysis and characterization of the surface coatings in view of micro-nano-view scale are of great significance for evaluating the corrosion mechanism of SSBPs, and predicting the dissolution rate or residual life of SSBPs.

Acknowledgements

This work was financially supported by the National Natural Science Foundation of China (No. 51704017), the National Key Research and Development plan of China (No. 2018YFB1502403), and the Communication Program for Young Scientist in USTB (No. QNXM20210010).

Conflict of Interest

The authors declare no conflict of interest.

References

[1] Y. Wang, H. Yuan, A. Martinez, P. Hong, H. Xu, and F.R. Bockmiller, Polymer electrolyte membrane fuel cell and hydrogen station networks for automobiles: Status, technology, and perspectives, *Adv. Appl. Energy*, 2(2021), art. No. 100011.

[2] J. Rodríguez-Varela, I.L. Alonso-Lemus, O. Savadogo, and K. Palaniswamy, Overview: Current trends in green electrochemical energy conversion and storage, *J. Mater. Res.*, 36(2021), No. 20, p. 4071.

[3] Y. Luo, Y.H. Wu, B. Li, T.D. Mo, Y. Li, S.P. Feng, J.K. Qu, and P.K. Chu, Development and application of fuel cells in the automobile industry, *J. Energy Storage*, 42(2021), art. No. 103124.

[4] M.K. Debe, Electrocatalyst approaches and challenges for automotive fuel cells, *Nature*, 486(2012), No. 7401, p. 43.

[5] V. Mazumder, Y. Lee, and S.H. Sun, Recent development of active nanoparticle catalysts for fuel cell reactions, *Adv. Funct. Mater.*, 20(2010), No. 8, p. 1224.

[6] B. Smitha, S. Sridhar, and A.A. Khan, Solid polymer electrolyte membranes for fuel cell applications—A review, *J. Membr. Sci.*, 259(2005), No. 1-2, p. 10.
[7] S.D. Wu, W.M. Yang, H. Yan, X.H. Zuo, Z.B. Cao, H.Y. Li, M.N. Shi, and H.B. Chen, A review of modified metal bipolar plates for proton exchange membrane fuel cells, *Int. J. Hydrogen Energy*, 46(2021), No. 12, p. 8672.
[8] J. Bi, J.M. Yang, X.X. Liu, D.D. Wang, Z.Y. Yang, G.Y. Liu, and X.D. Wang, Development and evaluation of nitride coated titanium bipolar plates for PEM fuel cells, *Int. J. Hydrogen Energy*, 46(2021), No. 1, p. 1144.
[9] T. Stein and Y. Ein-Eli, Challenges and perspectives of metal-based proton exchange membrane's bipolar plates: Exploring durability and longevity, *Energy Technol.*, 8(2020), No. 6, art. No. 2000007.
[10] R. Stroebel, *DOE Bipolar Plates Workshop Approach to Provide a Metallic Bipolar Plate Module to the Industry*, DOE bipolar plate workshop, Michigan [2017-02-14]. https://www.energy.gov/sites/prod/files/2017/05/f34/fcto_biploar_plates_wkshp_stroebel.pdf
[11] A. Hermann, T. Chaudhuri, and P. Spagnol, Bipolar plates for PEM fuel cells: A review, *Int. J. Hydrogen Energy*, 30(2005), No. 12, p. 1297.
[12] P.Y. Yi, L.F. Peng, T. Zhou, J.Q. Huang, and X.M. Lai, Composition optimization of multilayered chromium-nitride-carbon film on 316L stainless steel as bipolar plates for proton exchange membrane fuel cells, *J. Power Sources*, 236(2013), p. 47.
[13] C.H. Shen, M. Pan, Q. Yuan, and R.Z. Yuan, Studies on preparation and performance of sodium silicate/graphite conductive composites, *J. Compos. Mater.*, 40(2006), No. 9, p. 839.
[14] H.C. Kuan, C.C.M. Ma, K.H. Chen, and S.M. Chen, Preparation, electrical, mechanical and thermal properties of composite bipolar plate for a fuel cell, *J. Power Sources*, 134(2004), No. 1, p. 7.
[15] J. Wind, R. Späh, W. Kaiser, and G. Böhm, Metallic bipolar plates for PEM fuel cells, *J. Power Sources*, 105(2002), No. 2, p. 256.
[16] W. Yoon, X.Y. Huang, P. Fazzino, K.L. Reifsnider, and M.A. Akkaoui, Evaluation of coated metallic bipolar plates for polymer electrolyte membrane fuel cells, *J. Power Sources*, 179(2008), No. 1, p. 265.
[17] Y. Fu, M. Hou, G.Q. Lin, J.B. Hou, Z.G. Shao, and B.L. Yi, Coated 316L stainless steel with Cr_xN film as bipolar plate for PEMFC prepared by pulsed bias arc ion plating, *J. Power Sources*, 176(2008), No. 1, p. 282.
[18] Y.M. Xiong, S.L. Zhu, and F.H. Wang, Synergistic corrosion behavior of coated Ti60 alloys with NaCl deposit in moist air at elevated temperature, *Corros. Sci.*, 50(2008), No. 1, p. 15.
[19] L.J. Yang, H.J. Yu, L.J. Jiang, L. Zhu, X.Y. Jian, and Z, Wang, Graphite-polypyrrole coated 316L stainless steel as bipolar plates for proton exchange membrane fuel cells, *Int. J. Miner. Metall. Mater.*, 18(2011), No. 1, p. 53.
[20] V. Mehta and J.S. Cooper, Review and analysis of PEM fuel cell design and manufacturing, *J. Power Sources*, 114(2003), No. 1, p. 32.
[21] M.P. Brady, H. Wang, B. Yang, J.A. Turner, M. Bordignon, R. Molins, M.A. Elhamid, L. Lipp, and L.R. Walker, Growth of Cr-Nitrides on commercial Ni–Cr and Fe–Cr base alloys to protect PEMFC bipolar plates, *Int. J. Hydrogen Energy*, 32(2007), No. 16, p. 3778.
[22] Y. Wang, C.M. Wu, W. Li, H.Y. Li, Y.C. Li, X.Y. Zhang, and L.L. Sun, Effect of bionic hydrophobic structures on the corrosion performance of Fe-based amorphous metallic coatings, *Surf. Coat. Technol.*, 416(2021), art. No. 127176.
[23] R.A. Antunes, M.C.L. Oliveira, G. Ett, and V. Ett, Corrosion of metal bipolar plates for PEM fuel cells: A review, *Int. J. Hydrogen Energy*, 35(2010), No. 8, p. 3632.
[24] S.J. Lee, C.H. Huang, J.J. Lai, and Y.P. Chen, Corrosion-resistant component for PEM fuel cells, *J. Power Sources*, 131(2004), No. 1-2, p. 162.
[25] Q. Li, X. Lin, Q. Luo, Y.A. Chen, J.F. Wang, B. Jiang, and F.S. Pan, Kinetics of the hydrogen absorption and desorption processes of hydrogen storage alloys: A review, *Int. J. Miner. Metall. Mater.*, 29(2022), No. 1, p. 32.
[26] Y. Li, W.J. Meng, S. Swathirajan, S.J. Harris, and G.L. Doll, *Corrosion Resistant Pem Fuel Cell*, United States Patent, Appl. 5624769, 1997.
[27] C. Jirarungsatian and A. Prateepasen, Pitting and uniform corrosion source recognition using acoustic emission parameters, *Corros. Sci.*, 52(2010), No. 1, p. 187.
[28] Z.G. Chen, G.F. Zhang, and F. Bobaru, The Influence of passive film damage on pitting corrosion, *J. Electrochem. Soc.*, 163(2016), No. 2, p. C19.
[29] H.Y. Tian, L. Fan, Y.Z. Li, K. Pang, F.Z. Chu, X. Wang, and Z.Y. Cui, Effect of NH_4^+ on the pitting corrosion behavior of 316 stainless steel in the chloride environment, *J. Electroanal. Chem.*, 894(2021), art. No. 115368.
[30] N.B. Huang, C.H. Liang, and B.L. Yi, Corrosion resistance of PANi-coated steel in simulated PEMFC anodic environment, *Mater. Corros.*, 59(2008), No. 1, p. 21.
[31] J.C. Jiang, S.J. Liu, Z.Y. Ma, L.Y. Wang, and K. Wu, Butler-Volmer equation-based model and its implementation on state of power prediction of high-power lithium titanate batteries considering temperature effects, *Energy*, 117(2016), p. 58.
[32] G. Hinds and E. Brightman, *In situ* mapping of electrode potential in a PEM fuel cell, *Electrochem. Commun.*, 17(2012), p. 26.
[33] G. Hinds and E. Brightman, Towards more representative test methods for corrosion resistance of PEMFC metallic bipolar plates, *Int. J. Hydrogen Energy*, 40(2015), No. 6, p. 2785.
[34] J. Healy, C. Hayden, T. Xie, K. Olson, R. Waldo, M. Brundage, H. Gasteiger, and J. Abbott, Aspects of the chemical degradation of PFSA ionomers used in PEM fuel cells, *Fuel Cells*, 5(2005), No. 2, p. 302.
[35] A.M. Abdullah, A.M. Mohammad, T. Okajima, F. Kitamura, and T. Ohsaka, Effect of load, temperature and humidity on the pH of the water drained out from H_2/air polymer electrolyte membrane fuel cells, *J. Power Sources*, 190(2009), No. 2, p. 264.
[36] K.H. Hou, C.H. Lin, M.D. Ger, S.W. Shiah, and H.M. Chou, Analysis of the characterization of water produced from proton exchange membrane fuel cell (PEMFC) under different operating thermal conditions, *Int. J. Hydrogen Energy*, 37(2012), No. 4, p. 3890.
[37] X.Z. Wang, C.P. Ye, D.D. Shi, H.Q. Fan, and Q. Li, Potential polarization accelerated degradation of interfacial electrical conductivity for Au/TiN coated 316L SS bipolar plates used in polymer electrolyte membrane fuel cells, *Corros. Sci.*, 189(2021), art. No. 109624.
[38] M. Liu, H.F. Xu, J. Fu, and Y. Tian, Conductive and corrosion behaviors of silver-doped carbon-coated stainless steel as PEMFC bipolar plates, *Int. J. Miner. Metall. Mater.*, 23(2016), No. 7, p. 844.
[39] H.Q. Fan, D.D. Shi, X.Z. Wang, J.L. Luo, J.Y. Zhang, and Q. Li, Enhancing through-plane electrical conductivity by introducing Au microdots onto TiN coated metal bipolar plates of PEMFCs, *Int. J. Hydrogen Energy*, 45(2020), No. 53, p. 29442.
[40] D.W. DeBerry, Modification of the electrochemical and corrosion behavior of stainless steels with an electroactive coating, *J. Electrochem. Soc.*, 132(1985), No. 5, p. 1022.
[41] A.A. Hermas and M.S. Morad, A comparative study on the corrosion behaviour of 304 austenitic stainless steel in sulfamic and sulfuric acid solutions, *Corros. Sci.*, 50(2008), No. 9, p. 2710.

[42] J.S. Kim, W.H.A. Peelen, K. Hemmes, and R.C. Makkus, Effect of alloying elements on the contact resistance and the passivation behaviour of stainless steels, *Corros. Sci.*, 44(2002), No. 4, p. 635.
[43] R. Hornung and G. Kappelt, Bipolar plate materials development using Fe-based alloys for solid polymer fuel cells, *J. Power Sources*, 72(1998), No. 1, p. 20.
[44] X.W. Yuan, X. Wang, Y. Cao, and H.Y. Yang, Natural passivation behavior and its influence on chloride-induced corrosion resistance of stainless steel in simulated concrete pore solution, *J. Mater. Res. Technol.*, 9(2020), No. 6, p. 12378.
[45] E. Hamada, K. Yamada, M. Nagoshi, N. Makiishi, K. Sato, T. Ishii, K. Fukuda, S. Ishikawa, and T. Ujiro, Direct imaging of native passive film on stainless steel by aberration corrected STEM, *Corros. Sci.*, 52(2010), No. 12, p. 3851.
[46] X.Y. Wang, Y.S. Wu, L. Zhang, and B.F. Ding, Passivationm echanism of 316L stainless steel in oxidizing acid solution, *J. Univ. Sci. Technol. Beijing*, 7(2000), No. 3, p. 204.
[47] C.Y. Zhang, Y.H. Wei, J. Yang, W. Emori, and J. Li, Effects of nitric acid passivation on the corrosion behavior of $ZG_{06}Cr_{13}Ni_4Mo$ stainless steel in simulated marine atmosphere, *Mater. Corros.*, 71(2020), No. 9, p. 1576.
[48] Z.J. Lu and D.D. Macdonald, Transient growth and thinning of the barrier oxide layer on iron measured by real-time spectroscopic ellipsometry, *Electrochim. Acta*, 53(2008), No. 26, p. 7696.
[49] S. Habibzadeh, L. Li, D. Shum-Tim, E.C. Davis, and S. Omanovic, Electrochemical polishing as a 316L stainless steel surface treatment method: Towards the improvement of biocompatibility, *Corros. Sci.*, 87(2014), p. 89.
[50] W. Han and F.Z. Fang, Fundamental aspects and recent developments in electropolishing, *Int. J. Mach. Tools Manuf.*, 139(2019), p. 1.
[51] J. Richards, C. Cremers, P. Fischer, and K. Schmidt, Corrosion studies on electro polished stainless steels for the use as metallic bipolar plates in PEMFC applications, *Energy Procedia*, 20(2012), p. 324.
[52] S.J. Lee and J.J. Lai, The effects of electropolishing (EP) process parameters on corrosion resistance of 316L stainless steel, *J. Mater. Process. Technol.*, 140(2003), No. 1-3, p. 206.
[53] W. Han and F.Z. Fang, Two-step electropolishing of 316L stainless steel in a sulfuric acid-free electrolyte, *J. Mater. Process. Technol.*, 279(2020), art. No. 116558.
[54] A. Kumar, M. Ricketts, and S. Hirano, *Ex situ* evaluation of nanometer range gold coating on stainless steel substrate for automotive polymer electrolyte membrane fuel cell bipolar plate, *J. Power Sources*, 195(2010), No. 5, p. 1401.
[55] S.H. Wang, J. Peng, W.B. Lui, and J.S. Zhang, Performance of the gold-plated titanium bipolar plates for the light weight PEM fuel cells, *J. Power Sources*, 162(2006), No. 1, p. 486.
[56] X.J. Yan, J.B. Zhuang, N.B. Huang, C.H. Liang, H.T. Wang, and L.S. Xu, Corrosion behavior of SAMs modified silver-coated 316LSS as PEMFC bipolar plates, *Key Eng. Mater.*, 645-646(2015), p. 1233.
[57] H.L. Wang and J.A. Turner, Electrochemical nitridation of a stainless steel for PEMFC bipolar plates, *Int. J. Hydrogen Energy*, 36(2011), No. 20, p. 13008.
[58] S. Pugal Mani and N. Rajendran, Corrosion and interfacial contact resistance behavior of electrochemically nitrided 316L SS bipolar plates for proton exchange membrane fuel cells, *Energy*, 133(2017), p. 1050.
[59] D.M. Mattox, Physical vapor deposition (PVD) processes, *Met. Finish.*, 99(2001), p. 409.
[60] M. Aliofkhazraei and N. Ali, PVD technology in fabrication of micro- and nanostructured coatings, [in] *Comprehensive Materials Processing*, Elsevier, Amsterdam, 2014. p.49.
[61] N.S. Mansoor, A. Fattah-Alhosseini, H. Elmkhah, and A. Shishehian, Comparison of the mechanical properties and electrochemical behavior of TiN and CrN single-layer and CrN/TiN multi-layer coatings deposited by PVD method on a dental alloy, *Mater. Res. Express*, 6(2020), No. 12, art. No. 126433.
[62] S.H. Song, B.K. Min, M.H. Hong, and T.Y. Kwon, Application of a novel CVD TiN coating on a biomedical Co–Cr alloy: An evaluation of coating layer and substrate characteristics, *Materials*, 13(2020), No. 5, art. No. 1145.
[63] J.L. Wang, J.C. Sun, S. Li, Z.S. Wen, and S.J. Ji, Surface diffusion modification AISI 304SS stainless steel as bipolar plate material for proton exchange membrane fuel cell, *Int. J. Hydrogen Energy*, 37(2012), No. 1, p. 1140.
[64] D.G. Nam and H.C. Lee, Thermal nitridation of chromium electroplated AISI316L stainless steel for polymer electrolyte membrane fuel cell bipolar plate, *J. Power Sources*, 170(2007), No. 2, p. 268.
[65] Y. Hung, H. Tawfik, and D. Mahajan, Durability and characterization studies of polymer electrolyte membrane fuel cell's coated aluminum bipolar plates and membrane electrode assembly, *J. Power Sources*, 186(2009), No. 1, p. 123.
[66] A. Gago, A. Ansar, N. Wagner, J. Arnold, and K. Friedrich, Titanium coatings deposited by thermal spraying for bipolar plates of PEM electrolysers, [in] *The 64th Annual Meeting of the International Society of Electrochemistry*, Queretaro, 2013, p. 7.
[67] K.M. El-Khatib, M.O. Abou Helal, A.A. El-Moneim, and H. Tawfik, Corrosion stability of SUS316L HVOF sprayed coatings as lightweight bipolar plate materials in PEM fuel cells, *Anti-Corros. Methods Mater.*, 51(2004), No. 2, p. 136.
[68] H.B. Zhang, G.Q. Lin, M. Hou, L. Hu, Z.Y. Han, Y. Fu, Z.G. Shao, and B.L. Yi, CrN/Cr multilayer coating on 316L stainless steel as bipolar plates for proton exchange membrane fuel cells, *J. Power Sources*, 198(2012), p. 176.
[69] Y.J. Ren, C.R. Zhang, G.M. Liu, and C.L. Ceng, A review on corrosion and protection of metallic bipolar plates for proton exchange membrane fuel cell, *Corros. Sci. Protetion Technol.*, 21(2009), p. 388.
[70] Y. Fu, G.Q. Lin, M. Hou, B. Wu, Z.G. Shao, and B.L. Yi, Carbon-based films coated 316L stainless steel as bipolar plate for proton exchange membrane fuel cells, *Int. J. Hydrogen Energy*, 34(2009), No. 1, p. 405.
[71] K. Feng, Y. Shen, H.L. Sun, D.A. Liu, Q.Z. An, X. Cai, and P.K. Chu, Conductive amorphous carbon-coated 316L stainless steel as bipolar plates in polymer electrolyte membrane fuel cells, *Int. J. Hydrogen Energy*, 34(2009), No. 16, p. 6771.
[72] S.H. Lee, V.E. Pukha, V.E. Vinogradov, N. Kakati, S.H. Jee, S.B. Cho, and Y.S. Yoon, Nanocomposite-carbon coated at low-temperature: A new coating material for metallic bipolar plates of polymer electrolyte membrane fuel cells, *Int. J. Hydrogen Energy*, 38(2013), No. 33, p. 14284.
[73] L.X. Wang, J.C. Sun, P.B. Li, B. Jing, S. Li, Z.S. Wen, and S.J. Ji, Niobized AISI 304 stainless steel bipolar plate for proton exchange membrane fuel cell, *J. Power Sources*, 208(2012), p. 397.
[74] K.S. Weil, G. Xia, Z.G. Yang, and J.Y. Kim, Development of a niobium clad PEM fuel cell bipolar plate material, *Int. J. Hydrogen Energy*, 32(2007), No. 16, p. 3724.
[75] K. Feng, Z.G. Li, X. Cai, and P.K. Chu, Corrosion behavior and electrical conductivity of niobium implanted 316L stainless steel used as bipolar plates in polymer electrolyte membrane fuel cells, *Surf. Coat. Technol.*, 205(2010), No. 1, p. 85.
[76] K. Feng, Y. Shen, J.M. Mai, D.A. Liu, and X. Cai, An investigation into nickel implanted 316L stainless steel as a bipolar plate for PEM fuel cell, *J. Power Sources*, 182(2008), No. 1, p. 145.
[77] M.C. Li, S.Z. Luo, C.L. Zeng, J.N. Shen, H.C. Lin, and C.N. Cao, Corrosion behavior of TiN coated type 316 stainless steel

in simulated PEMFC environments, *Corros. Sci.*, 46(2004), No. 6, p. 1369.
[78] E.A. Cho, U.S. Jeon, S.A. Hong, I.H. Oh, and S.G. Kang, Performance of a 1 kW-class PEMFC stack using TiN-coated 316 stainless steel bipolar plates, *J. Power Sources*, 142(2005), No. 1-2, p. 177.
[79] Y. Wang and D.O. Northwood, An investigation into TiN-coated 316L stainless steel as a bipolar plate material for PEM fuel cells, *J. Power Sources*, 165(2007), No. 1, p. 293.
[80] Q.B. You, J. Xiong, T.N. Yang, T. Hua, Y.L. Huo, and J.B. Liu, Effect of cermet substrate characteristics on the microstructure and properties of TiAlN coatings, *Int. J. Miner. Metall. Mater.*, 29(2022), No. 3, p. 547.
[81] Y. Zhao, L. Wei, P.Y. Yi, and L.F. Peng, Influence of Cr–C film composition on electrical and corrosion properties of 316L stainless steel as bipolar plates for PEMFCs, *Int. J. Hydrogen Energy*, 41(2016), No. 2, p. 1142.
[82] T. Zhang and C.L. Zeng, Corrosion protection of 1Cr18Ni9Ti stainless steel by polypyrrole coatings in HCl aqueous solution, *Electrochim. Acta*, 50(2005), No. 24, p. 4721.
[83] S. Joseph, J.C. McClure, R. Chianelli, P. Pich, and P.J. Sebastian, Conducting polymer-coated stainless steel bipolar plates for proton exchange membrane fuel cells (PEMFC), *Int. J. Hydrogen Energy*, 30(2005), No. 12, p. 1339.
[84] M.A.L. García and M.A. Smit, Study of electrodeposited polypyrrole coatings for the corrosion protection of stainless steel bipolar plates for the PEM fuel cell, *J. Power Sources*, 158(2006), No. 1, p. 397.
[85] Y. Wang and D.O. Northwood, An investigation into polypyrrole-coated 316L stainless steel as a bipolar plate material for PEM fuel cells, *J. Power Sources*, 163(2006), No. 1, p. 500.